Biochimica et Biophysica Acta 1808 (2011) 1–18

Contents lists available at ScienceDirect

Biochimica et Biophysica Acta

journal homepage: www.elsevier.com/locate/bbamem

Review

A biophysical glance at the outer surface of the membrane transporter SGLT1 ☆

Navneet K. Tyagi [a,1,2], Theeraporn Puntheeranurak [a,b,2,3], Mobeen Raja [a,4], Azad Kumar [a,5], Barbara Wimmer [b], Isabel Neundlinger [b], Hermann Gruber [b], Peter Hinterdorfer [b], Rolf K.H. Kinne [a,*]

[a] Max Planck Institute of Molecular Physiology, Otto-Hahn-Strasse 11, D-44227 Dortmund, Germany
[b] Institute for Biophysics, Johannes Kepler University of Linz, Altenbergerstr. 69, 4040 Linz, Austria

ARTICLE INFO

Article history:
Received 11 March 2010
Received in revised form 22 July 2010
Accepted 26 July 2010
Available online 6 August 2010

Keywords:
Membrane transporter
Sodium/D-glucose cotransporter 1
Atomic force microscopy
Substrate/ inhibitor tagged cantilever
Tryptophan scanning
Membrane topology

ABSTRACT

Proteins mediating the transport of solutes across the cell membrane control the intracellular conditions in which life can occur. Because of the particular arrangement of spanning a lipid bilayer and the many conformations required for their function, transport proteins pose significant obstacles for the investigation of their structure–function relation. Crystallographic studies, if available, define the transmembrane segments in a "frozen" state and do not provide information on the dynamics of the extramembranous loops, which are similarly evolutionary conserved and thus as functionally important as the other parts of the protein. The current review presents biophysical methods that can shed light on the dynamics of transporters in the membrane. The techniques that are presented in some detail are single-molecule recognition atomic force microscopy and tryptophan scanning, which can report on the positioning of the loops and on conformational changes at the outer surface. Studies on a variety of symporters are discussed, which use gradients of sodium or protons as energy source to translocate (mainly organic) solutes against their concentration gradients into or out of the cells. Primarily, investigations of the sodium–glucose cotransporter SGLT1 are used as examples for this biophysical approach to understand transporter function.

Contents

☆ Dedicated in loving memory to Prof. Dr. Evamaria Kinne-Saffran.

* Corresponding author. Tel.: +1 212 395 9760; fax: +1 212 395 9760.
E-mail address: rolf.kinne@mpi-dortmund.mpg.de (R.K.H. Kinne).
[1] Present address: Howard Hughes Medical Institute, and Department of Genetics, Boyer Center, Yale School of Medicine, New Haven, CT 06511, USA.
[2] These authors contributed equally to this review.
[3] Present address: Department of Biology, Faculty of Science, Mahidol University, and Center of Excellence, National Nanotechnology Center at Mahidol University, Bangkok, 10400, Thailand.
[4] Present address: School of Molecular and Systems Medicine, 6126 HRIF East, Alberta Diabetes Institute, University of Alberta, Edmonton, Alberta, Canada T6G 2E1.
[5] Present address: Cell Biology and Gene Expression Unit, Laboratory of Neurogenetics, National Institute on Aging, National Institutes of Health, Bethesda, MD 20892, USA.

0005-2736/$ – see front matter © 2010 Elsevier B.V. All rights reserved.
doi:10.1016/j.bbamem.2010.07.028

1. Introduction

Transport proteins play an essential role in biology. As soon as the first unicellular organisms enwrapped in a cell membrane emerged, the control of solute traffic across the cell barrier became of utmost importance. This importance is reflected in the fact that about 25% of the genome is predicted to code for proteins involved in transmembrane transport [1]. The transport of a solute can either be active, when it occurs against an electrochemical gradient, or passive following the gradient. In turn, active transport can be achieved by so-called primary active transport where, as in the case of the various ATPases, chemical energy is used directly to energize the translocation of ions. Secondary active transport systems use the ion gradients established by the primary active transport systems via cotransport (symport and antiport) for the accumulation of other solutes.

One of these symport systems is the sodium-D-glucose cotransporter (SGLT) found as early as in *Vibrio* and essential for nutrient uptake in mammals [2]. There it serves as the mechanism by which D-glucose is taken up into the body in the small intestine; in the kidney two different SGLTs recover D-glucose filtered in the glomerulus from the primary urine and prevent loss of the carbohydrate [3]. Major breakthroughs in the understanding of the mechanisms of transport and in the molecular basis of transport of SGLT are the expression cloning by the group of Ernest Wright [4] and, most recently, the crystallization and the structural analysis of the *Vibrio* transporter by Faham et al. [5].

Membrane transporters are peculiar in their function in that during the translocation of a solute they undergo a cycle of conformational changes. In the outside orientation in the case of the SGLT binding of sodium followed by the binding of glucose occurs, then an occluded state is postulated. This step is followed by a conformation where the solute is now accessible from the cytoplasmic space, and sodium and the sugar are released into the cell. The transporter finally assumes the outside orientation again. Recently, several transporters have been crystallized and possible detailed mechanisms of cotransport have been proposed [5–10].

Recently, Claxton et al. [11] identified ion/substrate-dependent conformational changes in bacterial homolog of neurotransmitter: sodium symporter LeuT by using site-directed spin labelling and electron paramagnetic resonance. Their results outline the Na^+-dependent formation of a dynamic outward-facing intermediate that exposes the primary substrate-binding site and the conformational changes that occlude this binding site upon subsequent binding of the leucine substrate. Furthermore, their studies demonstrate that the binding of the transport inhibitors induce structural changes that distinguish the resulting inhibited conformation from the Na^+/leucine-bound state. Applying the same technique on lactose permease (LacY), Smirnova et al. [12] identified sugar-binding-induced outward-facing conformation of the symporter; conformational cycle of ABC transporter MsbA [13] in liposome was also identified using double electron–electron resonance spectroscopy.

Another widespread appraoch to identify functionally important parts in membrane cotransporter proteins is the subsituted cysteine accessibility method (SCAM) [14]. Frillingos et al. [15] have extensively used the SCAM technique to identify different aspects of Lac permease cotransporter. SCAM can be used to identify functionally important sites as well as reveal and/or confirm secondary structural details, including the peri- or cytoplasmic orientation of acccessible sites. A functionally important region in the putative third extracellular linker (ECL-3) of the renal Na^+/Pi cotransporter (NaPi-IIa) was probed using SCAM [16], and results of this study provide a valuable structure–function insights into cotransport meachnism. SCAM is also widely used for the identification of functional aspects of differnet membrane proteins, namely, cyclic nucleotide-gated channel [17], acetylcholine receptor [18,19], *Plasmodium falciparum* equilibrative nucleoside transporter 1 (PfENT1) [20], and the serotonin transporter [21]. Using the Cys residue accessibility toward MTS in the putative sugar translocation pathway of SGLT1 in combination with electrophysiology and fluorescence measurements, Loo et al. [22,23] elegantly measured real-time conformational changes and charge movements. Their finding provides strong support for an alternating access mechanism for Na^+-driven cotransporters. They also successfully identified two different conformational states of transporter, Na^+-bound state (CNa_2), and Na^+/sugar-bound state (CNa_2S).

Electrophysiology is another importnat biophysical tool to elucidate dynamics of membrane transporters. By measuring the electrophysiological properties of hSGLT1 in the cut-open oocyte technique, Chen et al. [24] identified two time constants, tau 1 and tau 2, which correspond to two steps in the conformational change of the free carrier. Na^+-binding/debinding modulates the slow time constant (tau 1), and a voltage-independent slow conformational change of the free carrier accounts for the observed plateau value of 10 ms. In an electrophysiology study on rabbit Na^+/glucose cotransporter 1, Hazama et al. [25] have shown that SGLT1 exhibits a presteady-state current after step changes in membrane voltage in the absence of sugar. These currents reflect voltage-dependent processes involved in cotransport and provide insight on the partial reactions of the transport cycle. Simulations of a 6-state ordered kinetic model for rabbit Na^+/glucose cotransport indicate that charge movements are due to Na^+-binding/dissociation and a conformational change of the empty cotransporter. In a recent electrophysiology study on rabbit SGLT1 [26], Na^+ and voltage dependence of transient SGLT1 kinetics was reported. Using step changes in membrane potential, in the absence of glucose but with 100 or 10 mM Na^+, transient currents were measured, corresponding to binding/debinding of Na^+ and to conformational changes of the protein.

There is evidence from other transporters, e.g., γ-aminobutyric acid transporters and citrate/malate transporter CimH, showing that exposed surface loops can act as a binding region for organic substrates [27] or can form a reentrant pore-loop-like structure with the accessibility depending on the conformation of the transporter [28–30]. During recent years, therefore, our group and others have concentrated on methods that are able to report on the conformational changes of those areas not resolved in the crystallography studies to determine their contribution to transmembrane transport.

One of these methods is atomic force microscopy, which, in its basic form, can resolve surface structures at an atomic level. Such

"morphological" studies using AFM have provided interesting insights into shape and presence of pores or transporters, and further modifications of the method, reviewed elsewhere [31], revealed other important aspects of membrane proteins. Our group concentrated on the use of single-molecule recognition AFM, which combines specificity of the signal with the analysis of forces and dynamics [32]. Using this method, results were obtained with regard to the membrane topology of transporter subdomains and identification of the functional role of subdomains on the cell surface. The maximal resolution obtained at this level is an area represented by an array of about 30 amino acids.

To increase the resolution to the level of single amino acids, tryptophan fluorescence and its changes during the transport cycle were investigated. Here, the main breakthrough occurred when hSGLT1 could be expressed in *Pichia pastoris* and isolated in a pure form in significant amounts by Tyagi et al. [33]. Combined with the tryptophan scanning method, where defined areas of the transporter can be labelled, this allowed the location of substrate and inhibitor sites both within the protein and with regard to the membrane lipids. In addition, this method, also described in more detail in this review, proved successful in determining at the molecular level the conformational changes that occur when inhibitors bind to subdomains of the transporter. This information is important because, currently, attempts are made to develop compounds that inhibit reabsorption of sugar in the kidney as a new approach to control blood sugar and thereby treat diabetes [34].

2. Single-molecule recognition atomic force microscopy

Atomic force microscopy (AFM) is one of the most powerful tools in nanobiotechnology. It can resolve features and surface topography of native biomolecules at subnanometer resolution [35]. AFM can be used on any kind of surfaces; hence, the number of AFM applications in life sciences, materials science, physical science, and industry has exploded since it was invented in 1986 [36]. The popularity of AFM is due to a number of reasons, such as easily achievable high resolution, low cost, little sample preparation, three-dimensional information in real space, in situ observations, fluid imaging, temperature controls, environmental controls, etc.

2.1. Imaging techniques

The principle and operation of AFM have been described extensively [36]. Briefly, its principle is relatively simple. It works in a way similar to a stylus profiler. The primary difference is that in AFM, the probe forces on the surface are much smaller than those in a stylus profiler. A soft cantilever tip is brought in contact with a surface. The repulsive force from the surface applied on the tip bends the cantilever upwards. The amount of bending, measured by a laser spot reflected on a split photo detector, can be used to calculate the force. By keeping the force constant while scanning the tip across the surface, the vertical movement of the tip follows the surface profile and is recorded as the three-dimensional surface topography. The resolution of this method relies on the end radius of the cantilever tip; reducing the end radius to 1 nm achieves atomic-scale resolution on hard surfaces [37]. There are several AFM imaging modes available for specific purposes. In general, contact and dynamic modes (i.e., tapping mode, intermittent or magnetic AC mode) have been widely used. They differ mainly in the way of tip raster-scan over the surface. For soft biological samples, e.g., cells, tissues, proteins, lipid membranes, the dynamic mode is often preferable to achieve high-resolution and nondestructive imaging.

2.2. Interaction force experiments

With the potential of AFM to image surface structures at the molecular scale and to measure ultra-low (a few piconewtons) forces at high lateral resolution, AFM also offers a unique opportunity to detect molecular recognition between individual ligands and receptors at different experimental conditions [38,39]. Biochemical modification of the cantilever tips [40,41,42] has paved the way for detecting ligand–membrane protein interactions at the single-molecule level. This provides fundamental insights into molecular dynamics of biological processes, e.g., the inter- and intramolecular interactions of biomolecules, and protein unfolding.

The principle of this technique is illustrated as a scheme of AFM force distance cycles in Fig. 1. The general strategy is to bind ligands to AFM tips and to probe sample or specimens for receptors on the surface. The ligands can be a specific antibody, a protein of interest, a substrate, or an inhibitor. The receptor can be a protein immobilized on various surfaces such as mica, glass, silicon, etc., or it can be a protein expressed on membranes of living cells. In a force–distance cycle (Fig. 1), the tip tagged with the ligand is first approached towards the surface whereupon a single receptor–ligand complex is formed based on the specific ligand–receptor recognition. During subsequent retraction of the tip from the surface, an increasing force is exerted on the ligand–receptor connection until the interaction bonds break at a critical force (unbinding force, f_u, calculated by using Hook's law $F = k\Delta x$, where k is the cantilever spring constant and Δx is the cantilever deflection). Such experiments allow to estimate affinity and rate constants and to define structural data of the binding pocket. In addition, they can be used to localize ligands and membrane receptors on biological surfaces [43–45]. In this review, we will describe how AFM can be used to explore the topology, conformational changes, and substrate–carrier interactions of the cotransporter SGLT1 protein in living cells on a single-molecule level.

2.3. Generation of antibody/substrate/inhibitor-tagged cantilevers

In single-molecule recognition AFM, the binding of ligand molecules (e.g., a specific antibody) to the AFM tip or to the surface is a critical step. This requires a careful AFM tip sensor design, including a firm attachment of the ligands to the tip surface at a low surface density. Moreover, the attached ligands should have enough mobility to interact with complementary molecules. To fulfil such goal, many kinds of ligand tip construction have been developed [46]. The recognition of ligands and its cognate molecule on the target surface is greatly facilitated by inserting a long, flexible poly (ethylene glycol) (PEG) chain between the tip and the probe molecule. The PEG spacer has several distinct advantages: PEG itself is a water-soluble, nontoxic, chemically and physically inert polymer, and the ligand can freely move and rotate around the tip within a restricted volume defined by the length of the cross-linker. Moreover, the nonlinear

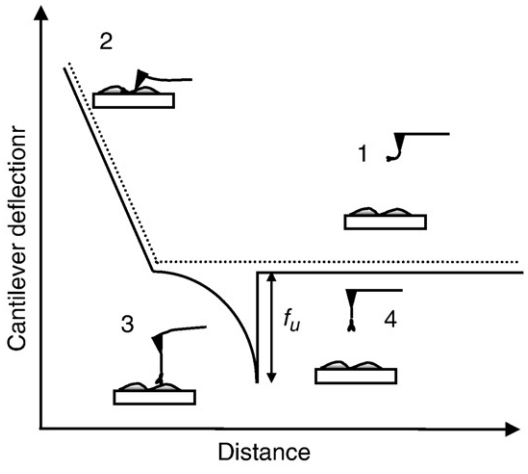

Fig. 1. AFM force distance cycle. Schematic representation of a force–distance cycle. The tip was moved toward the cell surface (dotted line, 1–2) and subsequently retracted (solid line) at a constant lateral position. During tip approach, the antibody forms a complex with an antigen which leads to a force signal of distinct shape (3) during tip retraction. The force increases until dissociation occurs (4) at an unbinding force (f_u). Reprinted with kind permission from Puntheeranurak et al. [49].

stretching behavior of the PEG tether helps to discriminate biospecific interactions from nonspecific tip–sample adhesion. Cross linker can vary in lengths. In our laboratory, we commonly used PEG linker of extended lengths of 6 nm; however, we recently also developed a longer cross-linker to probe deeper into transmembrane proteins.

To be able to react with the tip surface as well as the ligands the cross-linker is equipped with two different functional ends, i.e. one end couples to the tip and another end couples to the ligand. The heterobifunctional cross-linker widely used for protein (e.g., antibody) coupling has an *N*-hydroxy-succinimidyl (NHS) residue on the one end, which reacts to amines on the ethanolamine coated tip and a 2-pyridyldithiopropionyl (PDP) or a vinyl sulfon (VS) residue on the other end, which can covalently bind to thiols of ligands. This sulfur chemistry is highly advantageous, since it is very reactive and renders site-directed coupling possible. However, free thiols are hardly available on native ligands and must, therefore, be generated, e.g., by modification with SATP [*N*-succinimidyl-3-(*S*-acetylthio) propionate]. Other linkers widely used for protein coupling in our laboratory are the aldehyde-PEG_{800}-NHS and maleimide-PEG_{800}-NHS linkers, which interact with free amino groups of the peptide chains [41]. With these linkers, the need for prederivatization of nonthiol proteins is eliminated.

For our transporter experiments, the AFM tips were initially tagged with specific antibodies via PDP-PEG_{800}-NHS linkers, however, after the development of the aldehyde-PEG_{800}-NHS linker this one was used more frequently (Fig. 2A) [47,48]. In brief, AFM tips are first functionalized with ethanolamine by an overnight incubation with ethanolamine hydrochloride solubilized in Me_2SO. Then the aldehyde-PEG_{800}-NHS linker is covalently bound to amino groups on the tip surface. Next, the specific antibodies are coupled via the aldehyde function to the PEG-conjugated AFM tips. The tips are finally rinsed in the AFM working buffer and stored in the cold room. In glucose-binding experiments, the free SH group of 1-thio-β-D-glucose was coupled to the AFM tips via a VS-PEG-NHS linker or via newly developed acrylamide-PEG_{800}-NHS and acrylamide-PEG_{5000}-NHS linkers (Fig. 2B) [47,49]. The thio-glucose linked via a thio-glycosidic bond at the C1 position generates the 1-thio-D-glucose tip. Altogether, these methods use single-molecule tips, which contain a very low surface density of ligands (about 400 molecules/μm^2) on the tip surface to allow separate detection of single molecular events.

3. Tryptophan fluorescence

3.1. Intrinsic tryptophans

The aromatic amino acids tryptophan, tyrosine, and phenylalanine contribute to the intrinsic fluorescence of proteins. When all three residues are present in a protein, pure emission from tryptophan can be obtained only by photo selective excitation at wavelengths above 295 nm [50]. Although tyrosine and phenylalanine are natural fluorophores in proteins, tryptophan is the most extensively used amino acid

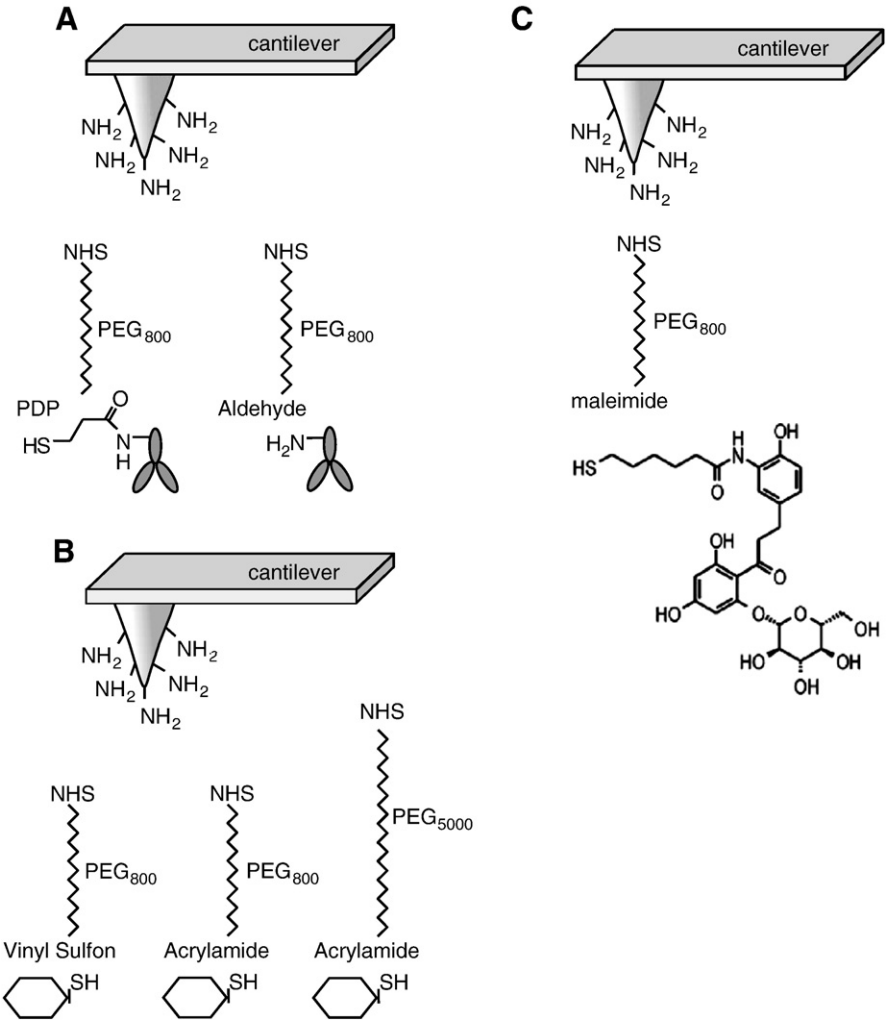

Fig. 2. Linkage of ligands to AFM tips. (A) Specific antibodies were covalently coupled to AFM tips via a heterobifunctional PEG derivatives, PDP-PEG_{800}-NHS (left) and aldehyde-PEG_{800}-NHS (right). (B) Sugars were covalently linked to AFM tips via vinyl sulfon-PEG_{800}-NHS (large end group) and acrylamide-PEG_{800} (and PEG_{5000})-NHS (small end group). (C) The maleimide-PEG_{800}-NHS was used to couple phlorizin to the AFM tips. The NHS end of the PEG linkers were covalently bound to amines on the functionalized tip surface.

for fluorescence analysis of proteins. In a protein containing all three fluorescent amino acids, observation of tyrosine and phenylalanine fluorescence is often complicated because of the interference by tryptophan resonance energy transfer [50,51]. Tryptophan residues serve as intrinsic, site-specific fluorescent probes for protein structure and dynamics [50] and are generally present at about 1 mol% in proteins [51]. The low tryptophan content of proteins is a favourable feature, which facilitates interpretation of fluorescence data and reduces complications due to intertryptophan interactions [52].

3.2. Tryptophan scanning

The well-documented sensitivity of tryptophan fluorescence to microenvironmental factors such as polarity makes tryptophan fluorescence a valuable tool in studies of protein structure and dynamics [50,51]. Thus, it has been documented that the position of the wavelength maximum of the fluorescence is shifted to a higher wavelength in a very hydrophilic environment and to a lower wavelength in more hydrophobic surroundings (see also Figs. 12 and 13). The presence of tryptophan residues as intrinsic fluorophores in most peptides and proteins makes them an obvious choice for fluorescence spectroscopic analysis. Tryptophans can be selectively introduced at various positions of the molecule (called tryptophan scanning). Thus, a peptide or protein can be mutated to replace critical amino acids by a tryptophan residue. This tryptophan then acts as a reporter group for any structural or conformational changes in the protein [53,54].

3.3. Quenching by hydrophobic and hydrophilic quenchers

Fluorescence quenching is operationally defined as a reduction in the measured fluorescence intensity when a fluorophore interacts with another molecule or group, called the quencher. After absorption of a photon, and before emission of radiation, a fluorescent molecule remains in its excited state for a short period, usually referred to as the excited state lifetime, which is typically in nanoseconds. If there is an interaction of a fluorophore in the excited state with a quencher, the excited fluorophore may be deactivated before emission of light can take place. The magnitude of quenching depends on the competition between the fluorescence process, the quenching process and other processes that lead to the deactivation of the excited state and are determined by their relative rates. The magnitude of quenching also depends on the concentration of the quencher, which determines the number of quencher molecules in close proximity to the fluorophore. Depending on the degree of intermolecular motion during the lifetime of the excited state, there can be two major quenching mechanisms: static and dynamic. Static quenching occurs when the distance between the fluorophore and quencher does not change during the lifetime of the excited state of the fluorophore. A special case of dynamic quenching occurs when the range of quenching interactions is sufficiently small so that only collisions between fluorophore and quencher result in quenching of fluorescence. This is called collisional quenching. The rate for such quenching processes is then limited by diffusion; in cases where quenching is efficient, this rate is the diffusion-controlled collision rate [50–52].

Hydrophobic compounds such as fatty acids, retinoids, or cholesteryl oleate diminish the fluorescence of some proteins. Analysis of the fluorescence data suggests that these proteins have a binding site for hydrophobic ligands [55]. Similarly, 2,2,2- trifluoroethanol is a useful hydrophobic quencher for proteins having predominantly tryptophan emission [56,57]. As will be detailed below, sodium-dependent D-glucose cotransport inhibitors that interact with SGLT1 via their hydrophobic moieties [53,54,58].

Quenching measurements employing small hydrophilic molecules such as potassium iodide (KI) and acrylamide (ACR) have been used successfully to study the accessibility of fluorescent groups in membrane proteins [51,53,54,58,59]. If at least one tryptophan residue is involved in direct substrate-binding or located in a segment undergoing domain transfer and/or conformational change, alterations are expected in protein fluorescence characteristics, i.e., emission wavelength, quantum yield, and/or susceptibility to quenching. By monitoring the intrinsic protein tryptophan emission and by measuring the relative abilities of KI and acrylamide to quench protein fluorescence in the presence of various ligands, we have now obtained further evidence for apparent conformational or positional changes that occur in this protein during D-glucose translocation or inhibitor binding [58].

Because the extent of fluorescence quenching depends on the accessibility of the fluorophore for the quencher, it has been very well utilized to explore the topology (surface or buried) of tryptophan residues in soluble proteins and peptides [53,54,60]. Another major application of fluorescence quenching has been to analyse penetration depths of membrane-bound proteins and peptides [61]. Membrane penetration depth is an important parameter in the study of membrane structure and organization. The depth of a group within a bilayer provides important information on topography, orientation and folding of membrane-bound proteins and peptides. In a typical quenching experiment using model membranes, a series of molecules labelled with quenchers that occupy different depths in the bilayer are incorporated into the membrane, which also contains the fluorophore of interest. The quenchers are often fatty acids or phospholipids with a quencher (spin label groups or heavy atoms such as bromine) covalently attached to the polar head group or to a specific fatty acyl carbon atom. This mode of attachment gives the quencher a relatively well-defined depth provided it does not loop back. In general, phospholipids labelled with quencher groups serve as better probes for such depth studies than quencher-labelled fatty acids for a number of reasons [62]. However, for studies involving native membranes, labelled fatty acids are preferred due to the relative ease of incorporation.

The quencher groups commonly used are dibromo or nitroxide derivatives. The quenching interactions for membrane-bound fluorophores and quenchers are predominantly static in nature with a typical quenching range of 8–12 Å [62–64]. The amount of quenching is determined from the ratio of fluorescence in a sample containing the quencher (defined as F) to that in a sample in which the quencher is omitted (defined as F_0). The pattern of variation of F/F_0 as a function of the depth of the quencher has been utilized to explore depths of penetration of tryptophan residues and other extrinsic fluorophores, e.g., in the nicotinic acetylcholine receptor [65], the haemolytic peptide melittin [66], cholesterol oxidase [67], the plant toxin ricin [68], the calcium-dependent membrane bound annexins [69], ion channels [70], and fusogenic peptides [71], signal sequence peptides [72], colicin [73], translocation proteins [74], Omp A protein [75], hSGLT1 [58], and C-terminal loop 13 of SGLT1 [76].

4. AFM studies of the binding domains under physiological conditions

4.1. Antibody-tagged cantilever

4.1.1. Membrane topology of the transporter

Several approaches have been used previously to determine the topology of the cotransporter SGLT1, for example computational algorithms, scanning mutagenesis, proteomics, and immunostaining methods [77–81]. For SGLT1 a model is proposed which contains 14 transmembrane α-helices and 13 surface domains or loops connecting the transmembrane segments (Fig. 3). However, the structural intramembrane topology of the SGLT1, especially of the large C-terminal loop connecting TMD 13 and 14, is still a matter of controversy [77–81]. An alternative way to probe the surface topology is to use AFM force spectroscopy [82]. The advantages of this approach are that one can probe unaltered cells, i.e. unfixed (living cells) under near-physiological conditions in terms of ion composition of the intra- and extracellular medium, membrane potential, and membrane fluidity. It is also important

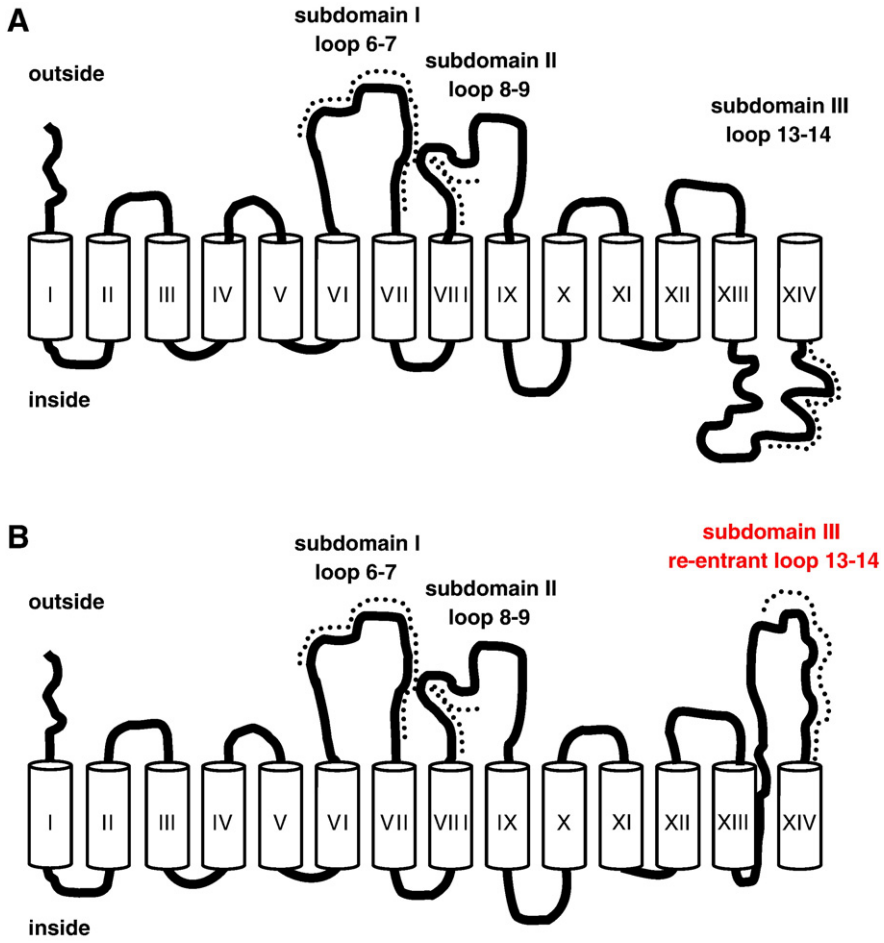

Fig. 3. Membrane topology of SGLT1. (A) Secondary structure proposed by Turk et al. [54]. The structure model shows 14 transmembrane helices with both the NH_2 and COOH termini facing the extracellular compartment. (B) Secondary structure modified according to the results obtained with the antibody-tagged AFM tips. Reprinted with kind permission from Puntheeranurak et al. [48].

to note that the transporters are not modified by mutagenesis, e.g. addition of glycosylation sites or tags; the latter can influence the protein orientation in the membrane. In addition, association of the transporter with other proteins inside the membrane, the cytoskeleton, and/or the cytoplasm is not likely to be disturbed. Thereby, three different antibodies (named QIS30, PAN2-2, and PAN3-2) against the three large extramembranous subdomains of SGLT1, i.e. subdomain I (loop 6–7), subdomain II (loop 8–9), and subdomain III (loop 13–14), respectively, were employed in single-molecule force spectroscopy experiments. The antibodies were separately coupled to AFM tips by using the heterobifunctional cross-linker as mentioned above. Force–distance cycles were performed at a fixed lateral position above the living cells, as described in Fig. 1, with the assistance of a CCD camera for the localization of the AFM cantilever on isolated cells or cell monolayers. The sweep–amplitude of the force–distance cycles was 1000 nm at a 1-Hz sweep rate. The typical specific recognition events from all three antibody-tagged AFM tips are shown in Figs. 4 and 5. Specificity of the recognition was confirmed by blocking experiments either by blocking the surface receptor with free antibodies or by blocking the AFM tip with free antigens. To achieve statistical significance, up to 500–1000 force–distance cycles were performed for each location on the surface of cells and up to four locations (different cells) were investigated for each experimental condition. From the results of these experiments, we could verify that subdomain I and subdomain II, as postulated from other studies, are located on the outer membrane surface of the transporter. In addition, we obtained evidence that at least the late part of subdomain III is also accessible from the extracellular space, suggesting a model for the membrane topology of the transport shown in Fig. 3, which contains a reentrant loop [48]. These results corroborate studies by the group from Gagnon et al. that have confirmed an extracellular orientation of the disputed loop 13–14 of SGLT1 using a different approach [79]. Immunohistochemistry and trypsin digestion analysis also support this finding [80,81 and Puntheeranurak et al. unpublished]. If one assumes that during substrate translocation by SGLT1 conformational changes occur, transmembrane helix 14 as a dynamic helical structure could alternate between inside-facing and outward-facing states, as previously reported for the *Escherichia coli* β-glucoside transporter BglF [83]. Thus, single-molecule AFM with antibody-tagged tip is a powerful tool for investigating topology of transporter and other membrane proteins.

4.1.2. Functional role of extracellular loops

Several studies of membrane transporters have proposed an important role of extracellular loops in facilitating substrate-binding and translocation [27–30]. For SGLT1 transporter, there are three large extramembranous loops that could be the site where the first interaction with the substrate occurs. The interaction between antibodies and their antigens is very sensitive to changes in the conformation of the latter. This phenomenon can be used to probe for conformational changes of subdomains during the catalytic transport cycle. The interaction of the various domains of SGLT1 with antibody-tagged cantilevers was therefore tested under conditions where the carrier is supposed to assume different translocation-related states.

First the state was induced in which a sodium–transporter complex is formed. Interestingly, as shown in Fig. 6, the presence of sodium did not alter the binding probability of any of the antibodies- suggesting only minor changes in the conformation of the three extracellular loops.

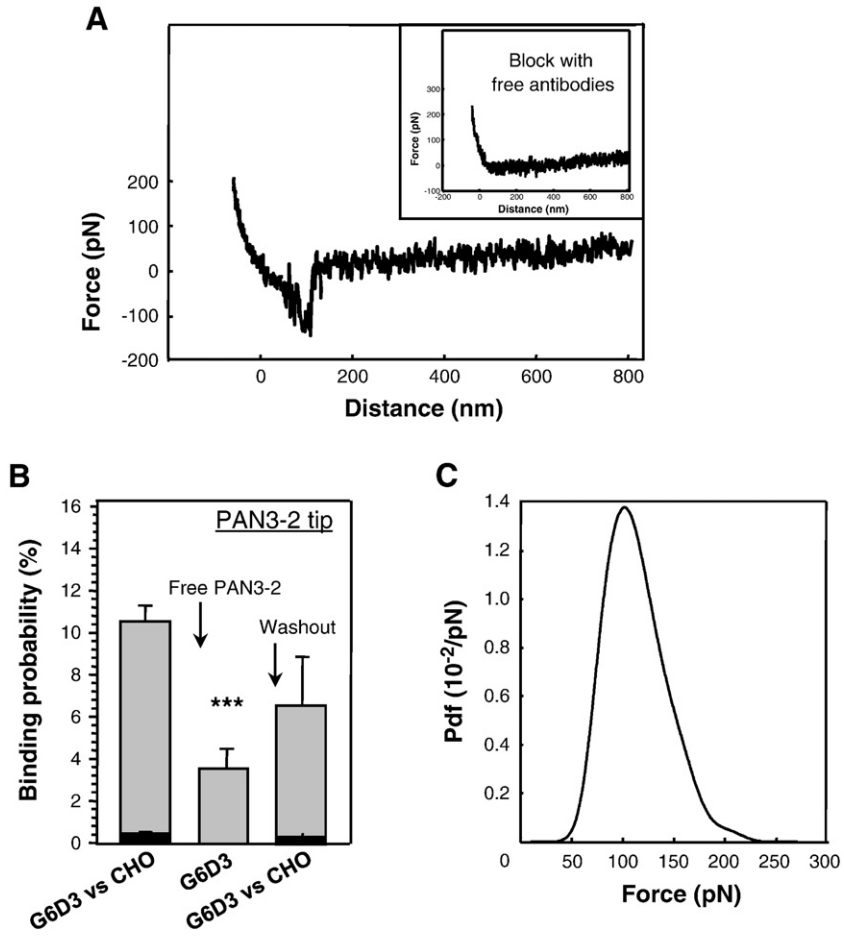

Fig. 4. Identification of SGLT1 on intact cells. Recognition of SGLT1 on the surface of intact cells by an AFM tip carrying an epitope specific antibody (PAN3-2). (A) Force curve showing specific interaction between the antibody and SGLT1 upon tip surface retraction. The specific interaction is blocked by injecting free PAN3-2 antibodies (0.3 μM) in the solution (inset). (B) Quantitative comparison of binding probabilities of PAN3-2-coated tips on SGLT1 expressing CHO cells (G6D3) (gray) and control CHO cells (black) in the absence or presence of free PAN3-2 in the medium. Values are mean ± SEM, $n = 2000–4000$, $P < 0.005$ compared with levels in the control group (unblocked). (C) Probability density function (PDF) giving the distribution of the unbinding force (f_u) of PAN3-2 to SGLT1 ($n = 1000$).

This result indicates that the conformational changes in the sodium-carrier complex observed using other biophysical approaches [22] occur inside the transporter and are not detectable in this part of the transporter surface. A significant change in the binding probability of the antibody directed to subdomain II was, however, observed when the interaction in the presence of the substrate D-glucose and sodium was tested (Fig. 6C). This indicates that during the formation of the sodium–glucose–carrier complex significant changes in the conformation of the transporter occur, which can be detected at the protein surface. Such changes were also observed measuring the intrinsic tryptophan

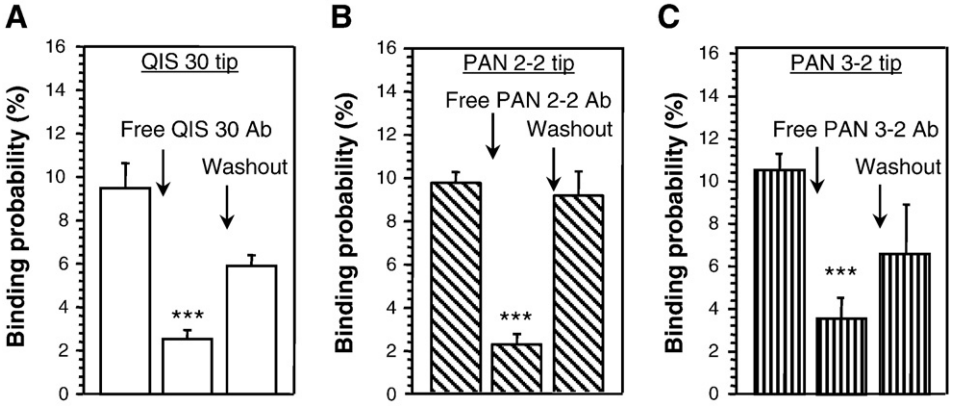

Fig. 5. Recognition of extramembranous loops of SGLT1 on the surface of intact cells by AFM tips tagged with epitope-specific antibodies (against subdomain I, II, and III). Quantitative comparison of binding probabilities of PAN3-2 (A), QIS30 (B), and PAN2-2 (C) antibodies, coupled to AFM tips to G6D3 cells in the absence or presence of free specific antibodies (3 μM) in the medium. Values are mean ± SEM (standard error of the mean), $n = 2000–4000$; $^{***}P < 0.005$ compared with levels in the relevant controls (absence of free antibodies in solution, value from the first bar). Reprinted with kind permission from Puntheeranurak et al. [48].

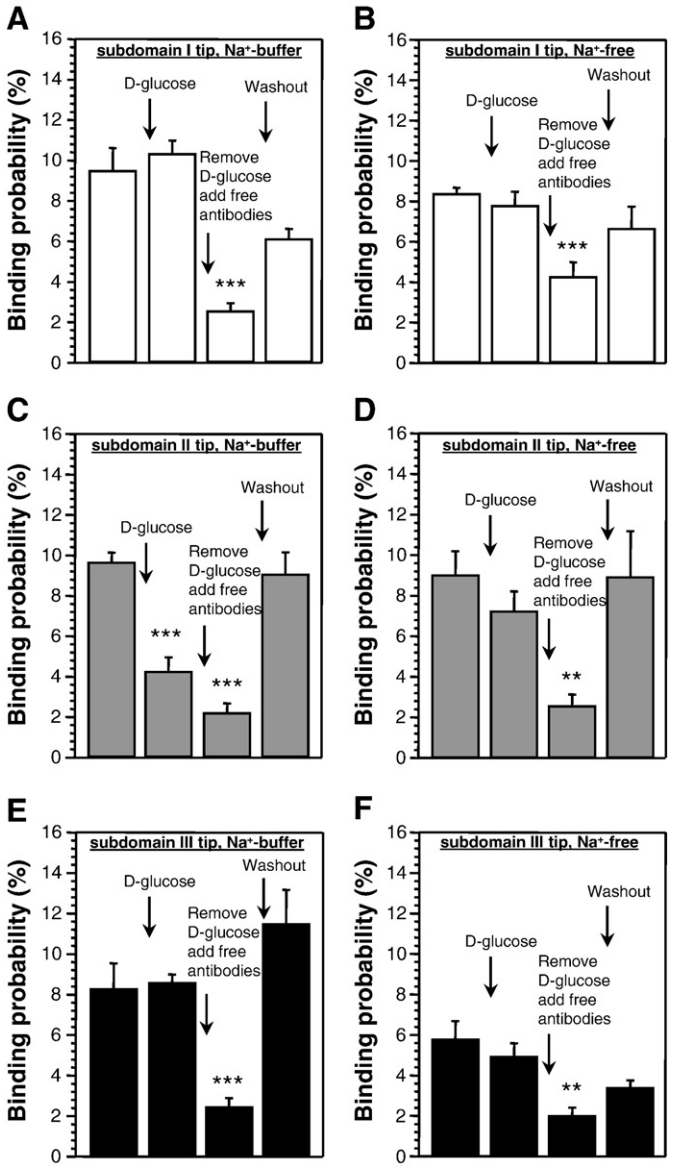

Fig. 6. Effect of D-glucose and Na^+ on the recognition of extramembranous loops of SGLT1 by antibodies. Effect of D-glucose on the binding probabilities of subdomain I (A, B), subdomain II (C, D), and subdomain III (E, F) antibody-tagged AFM tips to the surface of G6D3 cells in the presence of Na^+ (left row) and in the absence of Na^+ (right row). Values are mean ± SEM ($n = 1500–4000$; $^{**}P < 0.01$ and $^{***}P < 0.005$) compared with levels in the relevant controls (absence of 10 mM D-glucose or 3 μM antibodies, value from the first bar). Reprinted with kind permission from Puntheeranurak et al. [48].

fluorescence of the isolated transporter in solution [33] and in tryptophan fluorescence studies of the reconstituted transporter [84]. Additional studies involving site-directed mutagenesis of the cysteine residues located in this subdomain showed that the conformation of this loop critically influences the affinity of the transporter for D-glucose [48].

Furthermore, biochemical labelling studies and experiments testing the accessibility of the cysteines in the three loops suggest a disulfide bridge exists between loop 6–7 and loop 13–14. It is noteworthy in this context that different isoforms of SGLT1 exhibit individual properties in term of kinetics, substrate specificity, and inhibitor affinity [85]. Therefore, minor differences in the functional structure of different SGLT1 isoforms, particularly in the surface loops, might be expected. Irrespective what the exact partners are, such an intramolecular disulfide bridge would bring loop 6–7, loop 8–9, and loop 13–14 closer together. Thereby a vestibule of the transporter consisting of the three loops could be formed which contains the first site of interaction of the substrate with the transporter [48]. Biacore studies on the isolated loop 13 further support this assumption [86].

4.2. Substrate/inhibitor-tagged cantilever

4.2.1. Investigations on the initial sugar-binding site

Interaction of small ligands with proteins is required for translocation of the ligand itself, enzymatic reactions or regulation of the protein. SGLT1 is one of the proteins that undergo a series of conformational changes during the transport cycle [18–22]. Development of AFM and tip chemistry make it possible to couple small ligands such as 1-thio-glucose to the AFM tip, allowing for the first time to probe the glucose-binding site on SGLT1 in its native membrane incorporated state [47,49]. In this case, 1-thio-glucose-tagged AFM cantilevers (see above) were used to study the initial sugar-binding site. The experimental procedure was similar to the one employed with antibody-tagged AFM tips. The sugar is linked to the tip in such a way that the major recognition sites of the molecule (C2, C3, and C4) remain unaltered. The results illustrated in Fig. 7 shows that specific unbinding events of 1-thio-glucose to the SGLT1 transporter can be detected. The specific binding events were observed only in the presence of sodium and only on SGLT1-transfected CHO cells. The specificity of the interaction could also be confirmed by blocking the sugar-binding site with the potent inhibitor of SGLT1, phlorizin, (Fig. 7A) as well as blocking the transporter with a specific antibody [43]. Furthermore, the probability of binding was the same as that observed with the antibody-tagged cantilevers (see above). The average unbinding force of about 50 pN was smaller than that obtained with the antibodies (see Fig. 4), probably due to a lower affinity of the sugar to SGLT1. Since 1-thio-glucose is covalently attached to the cantilever tip and due to the bulkiness of the *p*-vinylsulfonylbenzoyl group present at the end of the linker (see above), it can be assumed that the sugar is not translocated, and only the site where the first interaction of the sugar with SGLT1 occurs is investigated. This offered the possibility to investigate the properties of this binding site in more detail. First of all, the binding site seems to be accessible only in the presence of sodium, thus suggesting that it is functionally active only when sodium is bound to the carrier. As a further characteristic, the substrate specificity of the binding site was investigated by blocking experiments using a variety of sugars. As expected, D-glucose (see Fig. 8) reduced the binding probability of the sugar-tagged cantilever—the same held for transported sugars such as D-galactose, α-methyl-D-glucoside (AMG), and 6-deoxy-D-glucose. L-glucose and 3-deoxy-D-glucose, sugars that are not transported, did not interact with the binding site, suggesting that a D-glucose configuration and a presence of an OH-group at C3 is required for the initial interaction with the carrier. Interestingly, 2-deoxy-D-glucose, also a nontransported sugar, prevented the interaction between the 1-thio-glucose-tagged cantilever and the carrier but inhibited only slightly AMG uptake. These results might suggest an initial binding site that represents a first selectivity filter that selects sugars with regard to D-or L-conformation and the presence or positioning of OH-groups at C1, C3, C4, and C6 but not at C2. The rejection of 2-deoxy-D-glucose has to occur later during a subsequent-binding/transport step. A similar discrepancy between initial binding and translocation has been observed previously in rat kidney proximal tubule. 2-Deoxy-D-glucose was shown to inhibit binding of phlorizin to isolated brush border membrane vesicles, but no transepithelial transport of the sugar was observed in microperfusion studies [87,88]. This raises the question why 2-deoxy-D-glucose does inhibit transport only slightly (if at all) but inhibits binding in the AFM and phlorizin-binding studies. In a model where the two steps binding and translocation are assumed to be sequential, equal inhibition of binding and transport should be observed. Apparently, in the presence of a large substituent at C1, such as the vinylsulfon group in the AFM studies or the two aromatic rings in phlorizin, the presence and positioning of the OH-group at C2 seems to become irrelevant for the binding reaction, thus both D-glucose and 2-deoxy-D-glucose act as inhibitors, based on

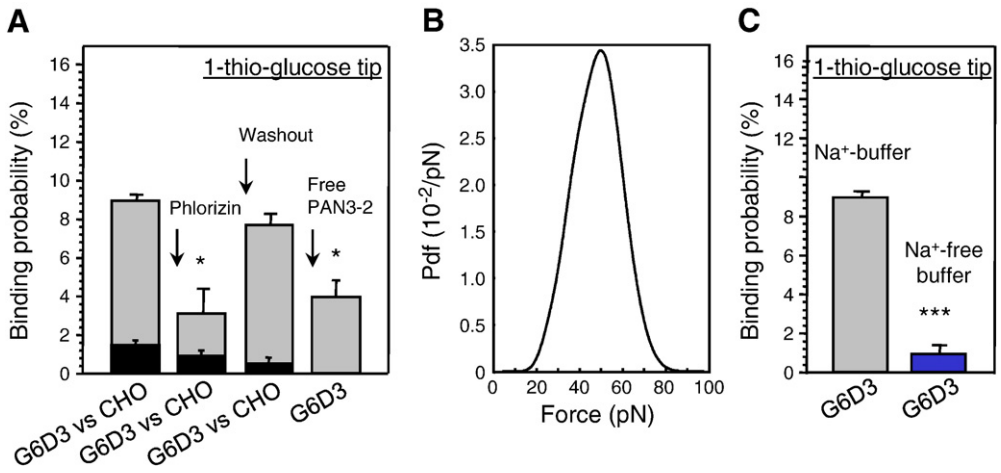

Fig. 7. Recognition of SGLT1 on the surface of intact cells by a 1-thio-glucose-tagged AFM tip. (A) The effect of phlorizin (0.5 mM) and the antibody PAN3-2 (3 μM) in the presence of Na^+ (KRH-NaCl) on the binding probabilities of 1-thio-glucose tip on G6D3 (gray) and CHO cells (black). (B) Probability density function (PDF) giving the distribution of the unbinding force f_u required to disrupt single glucose–receptor interaction ($n = 1000$). (C) Binding probabilities of 1-thio-glucose-tagged tip to G6D3 cells in the presence of Na^+ (gray) and in the absence of Na^+ (sodium replaced by *N*-glucosamine) (blue), respectively. Values are mean ± SEM, $n = 2000–4000$. $^*P < 0.05$ and $^{***}P < 0.005$ compared with levels in the control group (unblocked).

the presence of the OH-groups at C3, C4, and C6. This might be due either to conformational changes and sterical hindrances at the glucose molecule itself or to similar events at the transporter. In the absence of a large substituent (and as a free sugar) like in the AMG uptake studies, rejection of 2-deoxy-D-glucose as a substrate probably occurs already at the early binding site, and thus, the subsequent transport is not inhibited. Similar considerations seem not to apply to the OH-group at C3, which is further removed from the C1 position because 3-deoxy-D-glucose inhibits neither binding nor transport to a significant extent.

To reach the translocation site that is located deeper within the transporter, other linkers such as acrylamide-PEG_{800}-NHS and acrylamide-PEG_{5000}-NHS were used to couple the sugar to the AFM tips. These linkers are longer, and the acrylamide end group is less bulky and smaller than the *p*-vinylsulfonylbenzoyl group at the end of the linker. When scanning SGLT1-expressing cells with AFM tips tagged with these linkers, specific binding events could be observed in a comparable probability. The main difference between the various linkers is the increase in unbinding force found for the long acrylamide linker that probably arises from additional interactions of the sugar with transmembrane parts of SGLT1 [32]. Therefore, such long cross-linker might be promising candidates for studying the translocation pathways of transport proteins.

4.2.2. Investigations on the inhibitor-binding site

Inhibitors of SGLT have been recently become the focus of pharmaceutical and therapeutic interest in an attempt to find substances that block glucose absorption in the intestine or glucose reabsorption in the kidney [34]. Thus, a detailed understanding of the interaction between inhibitors and the transporter is desirable. A "classic" inhibitor of the transporter is phlorizin, a β-glycoside derived from the bark of apple tree roots. It is known to inhibit sodium-dependent sugar transport with a high affinity, the K_i being about one thousand fold lower than the K_m for glucose translocation [89].

For this purpose, amino-phlorizin was synthesized by a modification of a previously published method [Neundlinger et al., unpublished]. Amino-phlorizin was coupled to the AFM tip via C3 of the aromatic ring B extended with a 6-mercaptohexanoic acid spacer to PEG_{1300}-maleimide (see Fig. 2C). This coupling chemistry facilitated an ideal orientation for binding to the transporter as the major binding sites of phlorizin, the 2-,3-,4-, and 6-hydroxyl group of the pyranose ring and the 4′-OH and 6′-OH of the adjacent aromatic ring A are free to interact with SGLT1 [90]. We observed distinct recognition events between amino phlorizin-tagged cantilevers and SGLT1 expressed on the plasma membrane of living cells. Specificity of the interactions could be confirmed by masking the phlorizin-binding site with free phlorizin. Additionally, no significant-binding events were observed when parental CHO cells not expressing SGLT1 were probed [Neundlinger et al., unpublished]. These results support previous observations by Wielert-Badt et al. [91], where iodo-aceto-phlorizin had been used to probe the interaction between phlorizin and SGLT1 on isolated brush border membrane vesicles by AFM force spectroscopy. Thus, the phlorizin-binding epitopes on SGLT1 were accessible in both experiments.

Dynamic force spectroscopy experiments in which the rate of scanning is systematically varied generate force spectra from which additional information on the size of binding pockets and affinities can be derived. The energy length scale of the binding pocket of amino phlorizin seemed to be larger than that of glucose; indicating that the energy landscape of the phlorizin-binding pocket is larger than that of glucose [Neundlinger et al., unpublished]. These results are in good agreement with previous studies where it was shown that phlorizin binds to SGLT1 via its sugar moiety as well as its aglucone (phloretin) moiety. It was supposed that first the sugar moiety of phlorizin binds to the transporter followed by the binding of the aglucone moiety to a hydrophobic part of the protein resulting in a larger binding pocket of phlorizin. Additionally, conformational changes induced by phlorizin were predicted to be different to the reordering induced by glucose [92–94]. The amino acids involved in glucose-binding and those involved additionally in binding of the aglucone can also be visualized in the tryptophan scanning experiments of the isolated carrier (see below).

The size of the binding sites has been estimated from modelling of various inhibitors into a pharmacophore model to be in the order of $17 \times 10 \times 7$ Å [90]. Thus about 170 $Å^2$, a rather small portion of the total transporter surface of about 2000 $Å^2$, are involved in the binding of phlorizin. Furthermore, a lower dissociation rate of phlorizin compared to glucose was found as expected from the higher affinity of phlorizin to SGLT1 which has been observed previously [Neundlinger et al., unpublished].

To identify the subdomain involved in phlorizin-binding, AFM studies with phlorizin-tagged cantilever were combined with the use of subdomain-specific antibodies. Antibodies against subdomain III (aa 606–630) were demonstrated to reduce the binding probability, suggesting that the approach of phlorizin to its binding site was hindered in the presence of the antibody. The role of this segment of the transporter and the conformational changes occurring during the formation of the binding site phlorizin complex will be discussed below.

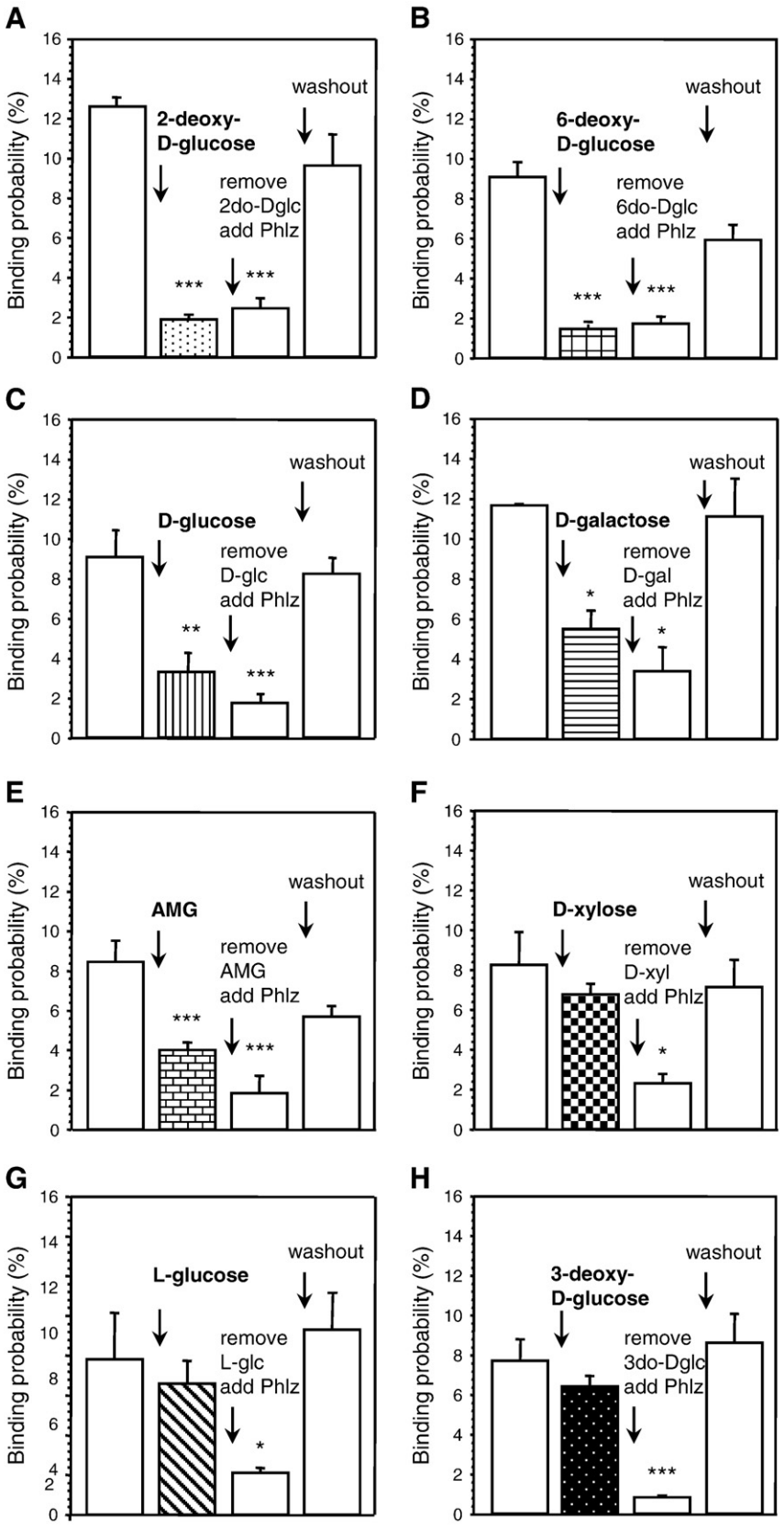

Fig. 8. Inhibition of initial D-glucose binding by various sugars. Binding probabilities of 1-thio-glucose tip and the effect of 2-deoxy-D-glucose (A, black-dotted bar), 6-deoxy-D-glucose (B, crossed bar), D-glucose (C, vertical-lined bar), D-galactose (D, horizontal-lined bar), AMG (E, bricked bar), D-xylose (F, chess bar), L-glucose (G, diagonal bar), and 3-deoxy-D-glucose (white-dotted bar) (10 mM each). Values are mean ± SEM, $n = 2000–4000$. 2do-Dglc, 2-deoxy-D-glucose; 6do-Dglc, 6-deoxy-D-glucose; D-glc, D-glucose; D-gal, D-galactose; AMG, α-methylglucoside; D-xyl, D-xylose; L-glc, L-glucose; 3do-Dglc, 3-deoxy-D-glucose; Phlz, phlorizin. $^{*}P < 0.05$, $^{**}P < 0.01$, and $^{***}P < 0.005$ compared with levels in the relevant controls (absence of sugars or phlorizin in solution, value from the first bar). Reprinted with kind permission from Puntheeranurak et al. [49].

5. Tryptophan fluorescence

5.1. Positioning of tryptophans in the intact carrier in solution and reconstituted in liposomes

The success in hSGLT1 expression and purification from *P. pastoris* [33] has opened a new avenue for different biophysical studies. Purified hSGLT1 in proteoliposomes exhibits substrate specificity in the following order: α-MDG > D-Glc ≈ D-Gal >> Man > All > L-Glc. The apparent K_m values for various sugars and the stereospecificity of recombinant hSGLT1 mirror those determined for hSGLT1 [95]. Catalytic turnover of hSGLT1 is 6 s^{-1}, which is in good agreement with that obtained in previous studies [95] and other Na^+-dependent transporters (e.g., the Na^+/glucose transporter of *Vibrio parahaemolyticus* [96], and Na^+/proline transporter of *Escherichia coli* [97]).

In the past 5 years, our group and others have utilized tryptophan-quenching techniques to explore unique features of transporters [33,58,84,98–101]. The location of the emission maximum of the combined fluorescence of the 14 tryptophans present in hSGLT1 suggests that, in detergent-containing solutions, the majority of tryptophans are located in a hydrophobic environment. This assumption is supported by the low accessibility of tryptophans to hydrophilic quenchers. Similar findings have been reported for other isolated membrane proteins such as the Na^+/galactose cotransporter of *V. parahaemolyticus* [99], lactose permease of *E. coli* [100], and P-glycoprotein multidrug transport transporter [101]. The same conclusion was reached in KI, acrylamide, and TCE-quenching studies of hSGLT1 in proteoliposomes, where most of tryptophan residues remain inaccessible to hydrophilic quenchers. However, in the presence of D-glucose, a tryptophan residue (or conceivably, fractional populations of several tryptophans) becomes located in a region which is more accessible to water due to conformational changes. This conformation is quite different from the one assumed by the carrier in the presence of phlorizin. Here a conformation prevails which is less compact, representing probably a more flexible state, which might prepare the transporter to execute the transmembrane translocation of the sugar and sodium ions [22].

Kumar et al. [84] also measured accessibility of the hSGLT1 tryptophans in solution and after reconstitution into liposomes by chemical modification using *n*-bromosuccinimide (NBS) as an oxidant (see Fig. 9). In the reconstituted state, even at a 50-fold molar excess of NBS, 75% of fluorescence was still observable, indicating that most of the tryptophan residues are inaccessible to chemical modification from the outside of the membrane. This result is in good agreement with the low degree of quenching exerted by the collisional quenchers. Quenching of hSGLT1 tryptophan fluorescence by NBS in solution shows a different pattern. In solution, approximately 35% of tryptophan residues in the transporter are deeply buried within the hydrophobic core of protein itself, since 65% of tryptophans are accessible for NBS oxidation compared to only 25% in the reconstituted form. These results clearly indicate that in a reconstituted form, about 40% of tryptophan residues are inaccessible for NBS modification due to their close contact with phospholipids and 35% tryptophan residues are buried deep inside the hydrophobic core of protein.

5.2. The sugar translocation and inhibitor-binding sites

One tryptophan scanning study of hSGLT1 from our group provides quite valuable information about the substrate recognition and inhibitor-binding sites in the cotransporter [54]. In this study, four single tryptophan residues (Q457W, T460W, F602W, and F609W) were separately introduced into a functional hSGLT1 mutant devoid of tryptophan residues (see Fig. 10). Trp457 and Trp460 mutants of hSGLT1 exhibit emission maxima at 343 and 340 nm, respectively, showing that the indole ring lies in a moderately hydrophilic environment. In mutants Trp457 and Trp460 D-glucose and phlorizin, but not the aglucone phloretin, quenched tryptophan fluorescence to the same extent (Figs. 10A and B). Both provide also protection against acrylamide, potassium iodide (KI), and trichloroethanol (TCE) quenching [58]. The parallax method (see details in hydrophobic quenching section) revealed an interfacial location for Gln457 at 10.8 Å and a deeper localization of Thr460 at 7.4 Å from the center of the bilayer; similar locations for these residues have been suggested in previous studies [77,78]. These results suggest that Gln457 and Thr460 are located in an area that forms part of the binding sites for D-glucose and for the sugar moiety of phlorizin (for a comparison with the vSGLT1 crystal structure, see Section 7).

The emission maxima for Trp602 and Trp609 mutants are in the range of 346–350 nm, which is typical for a very hydrophilic environment. Mutants Trp602 and Trp609 located in loop 13 exhibits in the presence of phlorizin a very strong quenching in fluorescence with 4–5 nm red shift in emission maxima (Figs. 10C and D). Both mutants also show protection against collisional quenchers in the presence of phlorizin and phloretin. These results indicate that Phe602 and Phe609 provide binding sites for the aglucone part of phlorizin (phloretin). Binding affinity of different ligands with hSGLT1 and its different single tryptophan mutants as determined by change in intrinsic tryptophan fluorescence exactly matched those determined by sugar uptake assay [58], indicating that the fluorescence changes occur at the sugar translocation site and not at the site of initial sugar binding identified above.

These results suggest that, in the native carrier, amino acids critically involved in sugar translocation reside in a hydrophilic access pathway extending 5–7 Å into the membrane. It is interesting to note that, from the crystal structure of various sodium-dependent transporters, a similar location of the sugar translocation site can be predicted [5] (see Fig. 11). To the same site, the sugar moiety of phlorizin is binding-extending about 5 Å into the transporter. This distance compares favourably with the depth of the binding pocket predicted from the pharmacophore studies [90]. The aglucone moiety of phlorizin interacts in addition strongly with Trp located in loop 13 at positions 602 and 609. This extramembranous loop had already been identified in mutagenesis studies as a region critically involved in phlorizin binding [102].

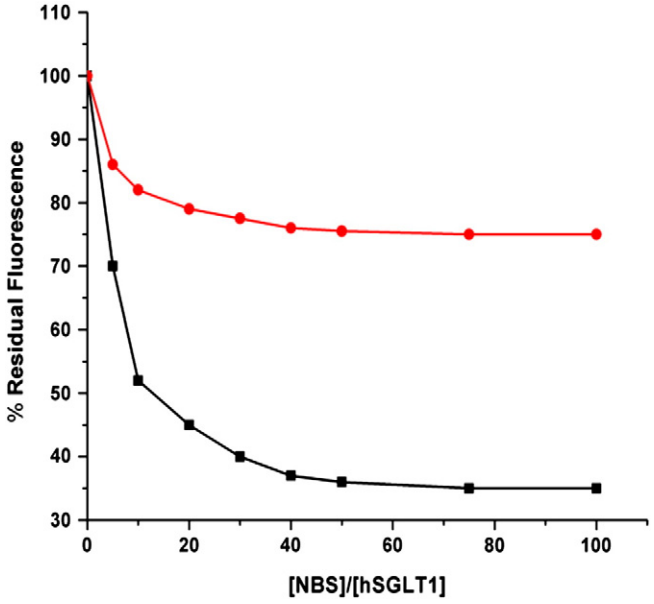

Fig. 9. NBS modification of hSGLT1 Trp residues in solution (■), and after reconstitution in proteoliposomes (●). 1 μM hSGLT1 in solution or in reconstituted in proteoliposomes in the lipid–protein ratio of 200:1 was subjected to NBS modification using 5-, 10-, 20-, 30-, 40-, 50-, 75-, and 100-fold molar excess of NBS over the transporter using a 2 mM stock solution of NBS in buffer. The decrease in emission intensity at 338 nm was monitored after 5 min of NBS addition, excitation wavelength used was 295 nm. A plot of the percent residual fluorescence at equilibrium (5 min) as a function of molar ratio of NBS/hSGLT1 is shown. Reprinted with kind permission from Kumar et al. [84].

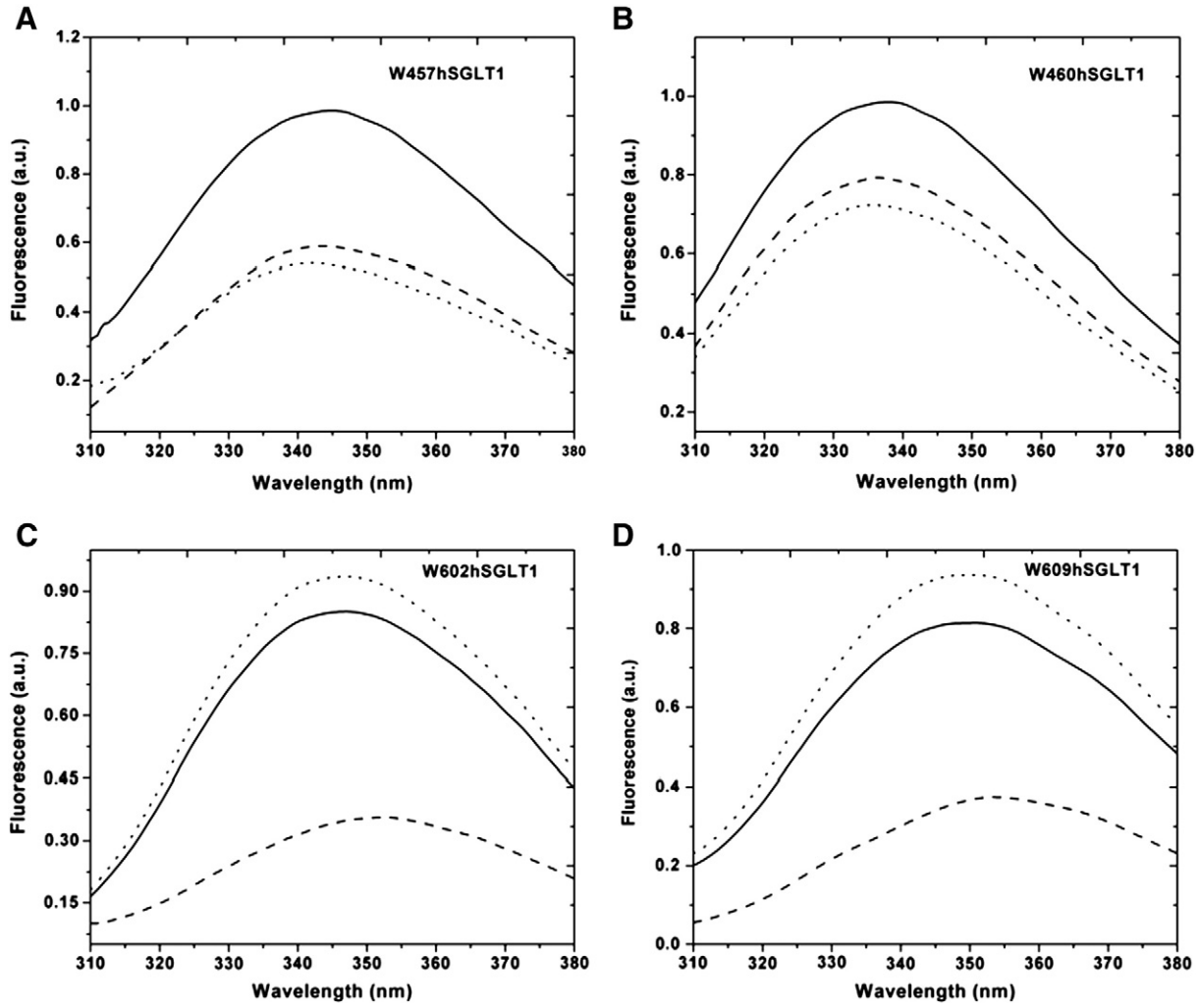

Fig. 10. Changes of fluorescence induced by D-glucose and phlorizin at different domains of hSGLT1 labelled with Trp. Transporters containing only one Trp at a defined position were isolated and incorporated into liposomes. Corrected emission spectrum of (A) W457hSGLT1, (B) W460hSGLT1, (C) W602hSGLT1, and (D) W609hSGLT1. For each experiment, 5 μM protein reconstituted into proteoliposomes in the ratio of 150:1 was incubated in the absence (solid line), presence of 10 mM D-glucose (dotted line), or presence of 100 μM phlorizin (dashed line). The excitation wavelength was 295 nm. The results shown are typical of ≈20 independent experiments. Reprinted with kind permission from Tyagi et al. [58].

Furthermore, antibodies against this domain inhibit binding of phlorizin-tagged cantilevers. Thus, the Trp fluorescence studies have added important information on the location of the sugar and phlorizin-binding site.

6. Biophysical studies on isolated subdomains of the carrier

6.1. Tryptophan fluorescence scanning studies on isolated loop 13 in solution

In view of the strong evidence that loop 13 is involved in the binding of phlorizin to the transporter, it became of interest to study the conformational changes induced by the inhibitor in more detail. For this purpose, several truncated loop 13 mutants were produced which contained one tryptophan at a defined position; therefore, the peptide could be scanned at every 10th amino acid position. Then the fluorescence spectrum and its changes by phlorizin as well as changes in accessibility of the tryptophan to hydrophilic quenchers were investigated [53].

Results of these experiments are shown in Fig. 12, which make it obvious that at each tryptophan position different movements of the peptide occur. From the shifts in the maximum, the decrease or increase in fluorescence and the changes in accessibility to hydrophilic quenchers the detailed model shown in Fig. 13 for the interaction at a molecular resolution could be obtained—defining acceptor as well as donor molecules of phlorizin and the peptide [53].

6.2. Biacore studies on isolated loop 13 reconstituted in lipid bilayers

Surface plasmon resonance (SPR) analysis is now widely used to study antibody–antigen, protein–protein, DNA–protein, DNA–DNA, and receptor–ligand interactions [103,104]. SPR analysis has been utilized to study binding of peptides to phospholipid membranes and to derive information regarding the membrane selectivity and structure–function relationship of antimicrobial peptides through binding affinity data [105].

We have also taken advantage of this technique to immobilize C-terminal loop 13 (aa 541–638) of SGLT1 on phospholipid bilayers and to demonstrate preservation of the native conformation and reactivity of this peptide [86]. Six histidine tags were introduced at both sides of the loop. The bilayers hydrophobic part as well as the space between the bottom sheet of the bilayer and the covalently bound dextran–matrix of the hydrophilic sensor chip appeared to facilitate incorporation of the whole loop 13 into the membrane [86]. This analysis confirmed the interaction of the loop with phlorizin, D-glucose, and L-glucose as well as the point of attachment of loop 13 via hydrophobic amino acids between aa 625 and 631, which, by measuring tryptophan fluorescence, had been shown previously to enter the lipid bilayer [77].

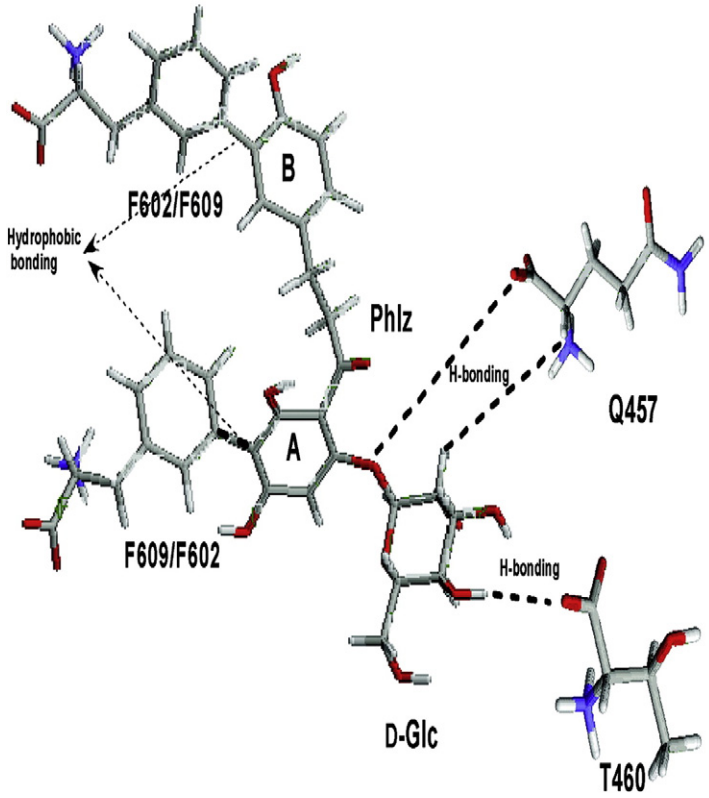

Fig. 11. Hypothetical scheme of major interaction sites between D-glucose and phlorizin with subdomains of hSGLT1. D-Glucose or the sugar moiety of phlorizin interact with residues Gln457and Thr460 present in transmembrane helix XI probably by the same hydrogen bonds; the aromatic ring A of the aglucone of phlorizin interacts with Phe609/Phe602, and ring B makes contact with Phe602/Phe609; both are present in the extramembranous loop 13 of hSGLT1. Reprinted with kind permission from Tyagi et al. [58].

7. Critical evaluation of our AFM and tryptophan fluorescence studies-based results in light of the available structural information of different transporters

The recently elucidated crystal structure of the solute sodium symporter family member sodium–galactose transporter (vSGLT) from *V. parahaemolyticus* [5] is a major advance toward understanding the structure–function relationship in this important class of transporters. The overall architecture has a maximal height and diameter of ~75 Å and ~55 Å (Fig. 14). There are 14 transmembrane helical segments (TM1 to TM14) with both N- and C-termini exposed to the periplasm. Most interestingly, vSGLT shared a common core structure of 10 transmembrane helices (TM1–10) with different gene families and symporters like LeuT, Mhp1, and BetP [8]. Although there is no sequence similarity between the internal repeat, they have a high degree of structural conservation permitting superimposition with each other.

The vSGLT structure is composed of a central group of seven helices (TM2, TM3, TM4, TM7, TM8, TM9, and TM11) that contribute side chain interactions for ligand selectivity, along with seven supporting helices that stabilize these central helices. A striking feature is the two discontinuous TM helices, TM2 and the symmetrically related TM7 helices, in the center of the protomer. In TM2, there is a break in the hydrogen-bonding pattern, dividing it into a roughly equivalent intracellular (TM2I) and extracellular (TM2E) components. In TM7, the helix is disrupted at residues F266, N267, Q268, and Y269, dividing it into a shorter intracellular (TM7I) and a larger extracellular (TM7E) segment. This structural feature may have particular functional importance as previously reported for several other cotransporters [106–108].

Topology of vSGLT and other symporters based on the available structural information show a seven helices inverted repeat core structure [8–10]. However, our topology model for SGLT1 based on AFM studies presented in this review is in stark contrast with inverted repeat idea. Possible explanation of this discrepancy might be the prokaryotic nature of vSGLT versus eukaryotic SGLT1 (rabbit) or the use of different experimental techniques, vSGLT in a frozen state versus SGLT1 expressed in G6D3 cells in a dynamic and fully functional form. However, it is also possible that our topology results represent the different conformational states of the transporter during a translocation cycle as previously observed in tryptophan fluorescence studies on hSGLT1 [33] and in electrophysiology studies on SGLT1 in *Xenopus* oocytes [22]. Presences of reentrant loop were also reported for the topology models for rat brain glutamate transporter [28,30] and citrate/malate transporter of *Bacillus subtilis* [29].

Faham et al. [5] determined that galactose is bound about half way across the membrane bilayer by specific side chain interactions from the central helices TM2E, TM3, TM7E, TM8, and TM11. The galactose-binding site is sandwiched between hydrophobic residues that form intracellular and extracellular gates. On the intracellular side, Y263 from the discontinuous helix TM7E stacks with the pyranose ring, a common feature seen in all sugar-binding structures to date [6,109]. This primary interaction, along with the flanking residues Y262, and W264, establishes a gate that prevents exit of sugar to the large hydrophilic cavity contiguous with the intracellular compartment. The extracellular gate is formed by a triad of hydrophobic residues (M73, Y87, and F424). Directly above the hydrophobic residues, there are substantial interactions between TM11, TM3, TM2E, and TM7E with the loops from TM2–TM3, TM8–TM9, and TM10–TM11. For the verification of structural data

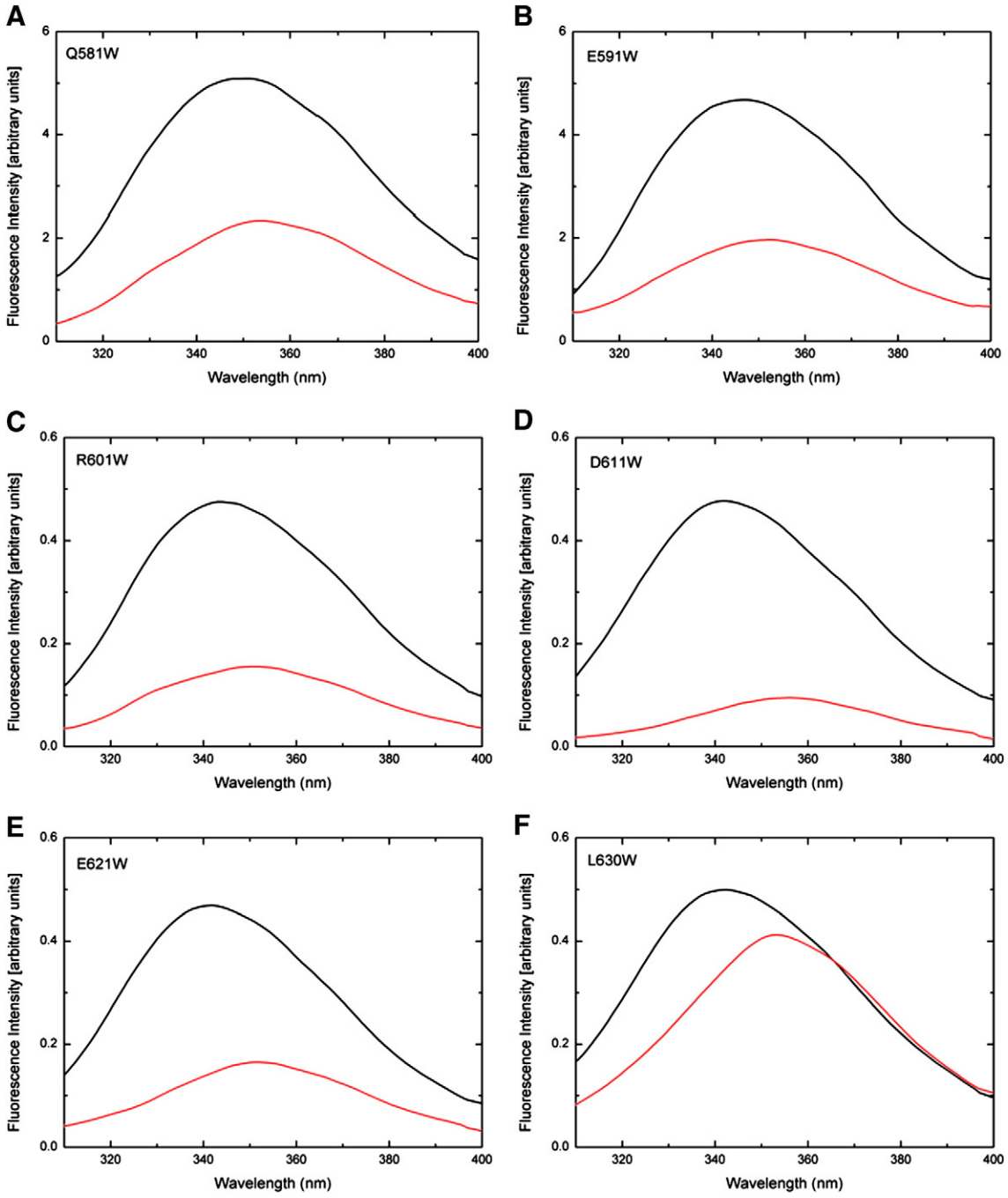

Fig. 12. Effect of phlorizin on fluorescence emission spectra of single Trp mutants of loop 13 in solution. The *dotted lines* show the corrected spectra, and the *solid lines* represent the effect of 100 μM phlorizin on the intrinsic fluorescence of each Trp mutant. The protein samples include (A) Q581W, (B) E591W, (C) R601W, (D) D611W, (E) E621W, and (F) L630W. Reprinted with kind permission from Raja et al. [53].

and to further understand the functional importance of different amino acids identified as potential substrate-binding partner, Faham et al. [5] mutated those amino acids into alanine and measured galactose transport in proteoliposomes. The Q69A, E88A, N260A, K294A, and Q428A mutations did not show Na^+-dependent galactose transport. In contrast, the S91A mutant behaved normally, which suggests that this amino acid is not essential for transporter function (S91 is not conserved across different species). Mutants of the corresponding sugar-binding sites in SGLT1 (K321A, Q457R, Q457C, and Q457W) provide strong support for the arguments that these residues also play an important role in the mammalian transporter [26,58,110]. In our tryptophan scanning studies [58], we also observed that the Q457W mutant shows a drastic change in the sugar transport properties and has lower affinities towards different substrates. Parallax method revealed a similar location for this residue as observed for the corresponding Q428 residue in vSGLT crystal structure. However, in our tryptophan scanning studies, we identified also residue T460 as a probable amino acid involved in sugar-binding/transport and inhibitor binding, which is in contrast to the vSGLT crystal structure. Probable reasons for discrepancy might be that this residue involved in sugar-binding/transport only transiently or in an indirect fashion. So far, no crystallographic information is available for SGLT1 in a phlorizin-bound state, so our tryptophan scanning results for the phlorizin-binding sites cannot be compared (yet) with structural data.

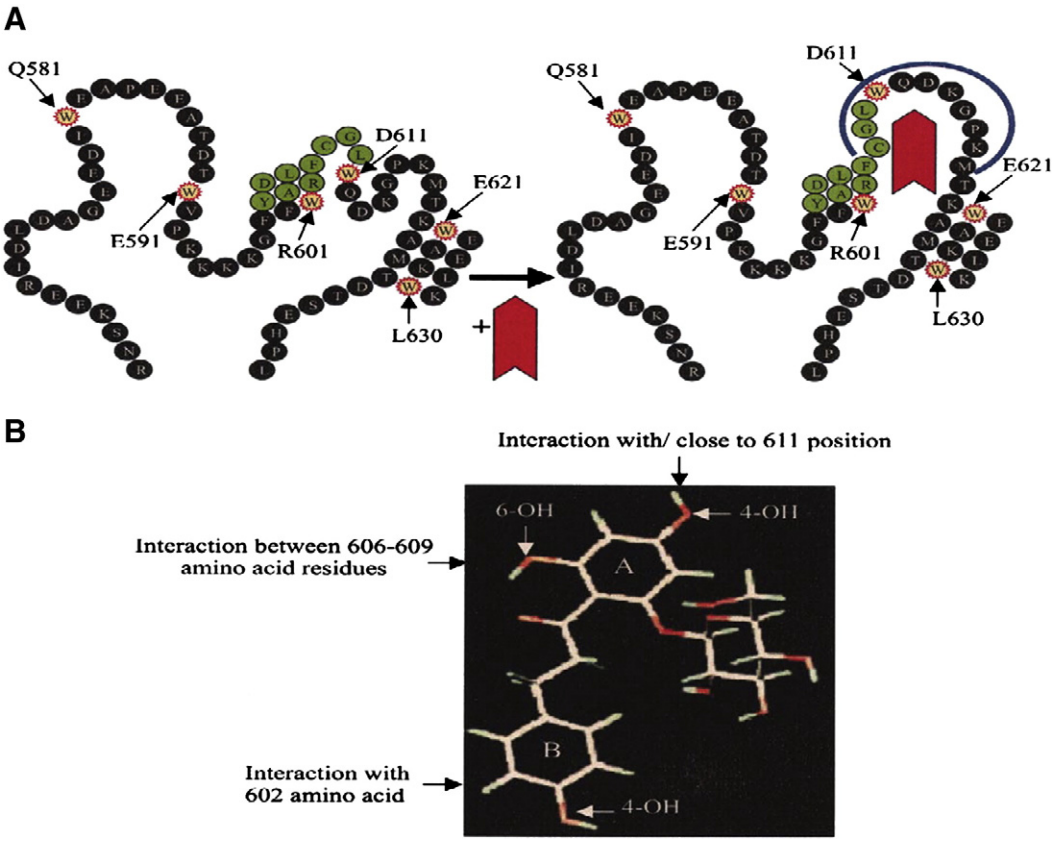

Fig. 13. A two-dimensional model of the interaction between loop 13 and phlorizin. (A) Two-dimensional model of truncated loop 13 of rabbit SGLT1 (amino acids 564–638). Left panel: arrangement of amino acids in the absence of phlorizin. α-Helical areas are based on a computer program; the arrangement of random coil takes into account the hydrophobicity of the tryptophan environment as predicted from the fluorescence maxima. Right panel: yellow represents the Trp mutations; green represents the presumed phlorizin-binding region; the red arrow indicates the proposed position of phlorizin in the binding region; and the blue arc highlights the main area of conformational changes. The exposure of the region around position 611 to a more hydrophilic environment is derived from the strong red shift in the tryptophan fluorescence maxima. (B) Three-dimensional conformation of phlorizin according to NMR studies by Wielert-Badt et al. [90]. The arrows show the interactions of aromatic ring A with the binding region. Reprinted with kind permission from Raja et al. [53].

Sodium is the ion driving substrate translocation in LeuT, vSGLT, Mhp1, and BetP [8]. For LeuT, vSGLT, and Mhp1, the sodium-binding site is located at the intersection of TM1 and TM8 ~ 8 Å away from the substrate-binding site. There appears to be a conserved coordination pattern made by carbonyl oxygens in the unwound segment of TM1 and hydroxyl groups from serine and/or threonine residues in TM8 [111]. Functional evidence for sodium-binding site in vSGLT is provided by the finding that mutation of S365 abolishes transport [5].

8. Synopsis

The aim of the studies presented above was to learn more about the role and dynamics of extramembranous loops of a transporter in substrate-binding and inhibitor interaction. For SGLT1, the following picture emerges. Extra membranous loops 6–7, 8–9, and the late part of loop 13–14 face the extracellular space. They have a tertiary structure defined by helical sections within the loops (in particular, loop 13) and the connections of the loops via disulfide linkages. This "vestibule" exhibits sufficient stability to act as the primary selectivity filter of the transporter. The site is normally occluded; access becomes only possible when sodium is bound to the carrier. The formation of the sodium–carrier complex causes conformational changes, which open the access to the sugar translocation site, buried about 5 Å deep in the protein. This might involve iris-like movements of scaffolding transmembrane helices as described for the betaine transporter [112]. The sugar can subsequently diffuse into the hydrophilic pocket and binds to the translocation site. The binding also alters the conformation of the vestibule—potentially to aid in the vectorial movement of the transportate through the carrier. The ensuing steps—transition from the *cis*- conformation into the *trans*-conformation which includes establishing of hydrophobic diffusion barriers at both sides of the transportate and subsequent opening of a hydrophilic pocket toward the cytoplasmic space—are well described in the crystallographic studies [5].

The extramembranous loops play also an important role in the binding of inhibitors to the transporter. For glycosidic inhibitors with aromatic or aliphatic aglucones they provide stereoselective recognition sites for the aglucones. The binding induces elaborate conformational changes in loop 13 which are transferred to the conformation of the transmembrane helices promoting a very condensed state of the transporter in which no translocation can occur.

Biophysical techniques thus provide tools to study the processes occurring at the surface of a transport protein, be it the outer surface by allowing determination of the topology, functional role, and conformational changes of extramembranous segments; be it by localizing and characterising processes taking place at the inner surfaces, the selectivity filters and the translocation sites of a transporter. Also, the interactions at the lipid–protein interfaces between the transporter and the membrane lipids can be investigated. These techniques allow us to investigate the transporter protein from a different perspective, which can strengthen the knowledge obtained by other means. Thus, biophysical methods present an important complementary approach in our aim to understand the structure–function relationship of those proteins which control the passage of solutes across the membranes of the cells, thereby providing the intracellular environment wherein life can exist.

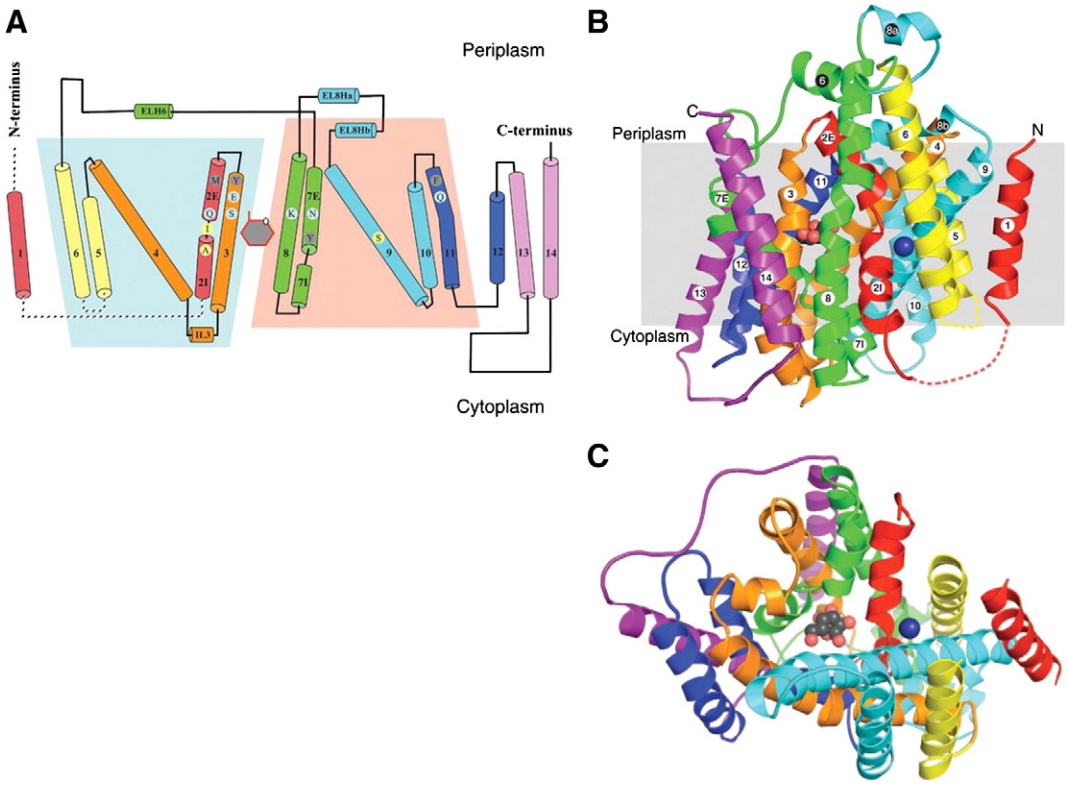

Fig. 14. Structure of vSGLT. (A) Topology. The structure is colored as a rainbow from the N terminus (red) to the C terminus (purple). The blue and red trapeziums represent the inverted topology of TM2 to TM6 and TM7 to TM11. The gray hexagon with red trim represents the galactose. Residues involved in sugar recognition, gate residues, and a proposed sodium binding site are shown in cyan, gray, and yellow circles. (B) Structure viewed in the membrane plane. The coloring format and numbering of α-helices is same as in panel A. (C) Structure viewed from the intracellular side. Reprinted with kind permission from Faham et al. [5].

Acknowledgments

The authors gratefully acknowledge the indispensable help of skilled technicians in performing the experiments, the valued intellectual support of junior and senior scientists in interpreting the results, and the dedication of highly efficient secretaries in publishing the studies. The joint efforts of the authors in Dortmund, Linz, New Haven, Bethesda, Alberta and Bangkok made writing this review a truly international experience.

References

[1] E.S. Lander, et al., Initial sequencing and analysis of human genome, Nature 409 (2001) 860–921.
[2] E.M. Wright, E. Turk, The sodium/glucose cotransport family SLC5, Pflugers Arch. 447 (2004) 510–518.
[3] E.M. Wright, M.G. Martin, E. Turk, Intestinal absorption in health and diseases—sugars, Best Pract. Res. Clin. Gasteroenterol. 17 (2003) 943–956.
[4] M.A. Hediger, M.J. Coady, T.S. Ikeda, E.M. Wright, Expression cloning and cDNA sequencing of the Na^+/glucose co-transporter, Nature 330 (1987) 379–381.
[5] S. Faham, et al., The crystal structure of a sodium galactose transporter reveals mechanistic insights into Na^+/sugar symport, Science 321 (2008) 810–814.
[6] J. Abramson, I. Smirnova, V. Kasho, G. Verner, H.R. Kaback, S. Iwata, Structure and mechanism of the lactose permease of *Escherichia coli*, Science 301 (2003) 610–615.
[7] P.L. Shaffer, A. Goehring, A. Shankaranarayanan, E. Gouaux, Structure and mechanism of a Na^+-independent amino acid transporter, Science 325 (2009) 1010–1014.
[8] J. Abramson, E.M. Wright, Structure and function of Na^+ symporters with inverted repeats, Curr. Opin. Struct. Biol. 19 (2009) 425–432.
[9] L.R. Forrest, G. Rudnick, The rocking bundle: a mechanism for ion-coupled solute flux by symmetrical transporters, Physiology 24 (2009) 377–386.
[10] H. Krishnamurthy, C.L. Piscitelli, E. Gouaux, Unlocking the molecular secrets of sodium-coupled transporters, Nature 459 (2009) 347–355.
[11] D.P. Claxton, M. Quick, L. Shi, F.D. de Carvalho, H. Weinstein, J.A. Javitch, H.S. McHaourab, Ion/substrate-dependent conformational dynamics of a bacterial homolog of neurotransmitter :sodium symporters, Nat Struct Mol Biol. 7 (7) (2010) 822–829.
[12] I. Smirnova, V. Kasho, J.Y. Choe, C. Altenbach, W.L. Hubbell, H.R. Kaback, Sugar binding induces an outward facing conformation of LacY, Proc. Natl. Acad. Sci. USA 104 (2007) 16504–16509.
[13] P. Zou, M. Bortolus, H.S. Mchaourab, Conformational cycle of the ABC transporter MsbA in liposomes: detailed analysis using double electron–electron resonance spectroscopy, J. Mol. Biol. 393 (2009) 586–597.
[14] A. Karlin, M.H. Akabas, Substituted-cysteine accessibility method, Methods Enzymol. 293 (1998) 123–145.
[15] S. Frillingos, M. Sahin-Toth, J. Wu, H.R. Kaback, Cys-scanning mutagenesis: a novel approach to structure–function relationships in polytopic membrane proteins, FASEB J. 13 (1998) 1281–1299.
[16] G. Lambert, I.C. Foster, G. Stange, K. Kohler, J. Biber, H. Murer, Cysteine mutagenesis reveals novel structure–function features within the predicted third extracellular loop of the type IIa Na^+/Pi cotransporter, J. Gen. Physiol. 117 (2001) 533–546.
[17] Z.P. Sun, M.H. Akabas, E.H. Goulding, A. Karlin, S.A. Siegelbaum, Exposure of residues in the cyclic nucleotide-gated channel pore: P region structure and function in gating, Neuron 16 (1996) 141–149.
[18] M.H. Akabas, D.A. Stauffer, M. Xu, A. Karlin, Acetylcholine receptor channel structure probed in cysteine-substitution mutants, Science 258 (1992) 307–310.
[19] A. Karlin, M.H. Akabas, Toward a structural basis for the function of nicotinic acetylcholine receptors and their cousins. Neuron 15 (6) (1995) 1231–1244.
[20] P.M. Riegelhaupt, I.J. Frame, M.H. Akabas, Transmembrane segment 11 appears to line the purine permeation pathway of the *Plasmodium falciparum* equilibrative nucleoside transporter 1 (PfENT1), J. Biol. Chem. 285 (2010) 17001–17010.
[21] M.I. Torres-Altoro, C.P. Kuntz, D.E. Nichols, E.L. Barker, Structural analysis of the extracellular entrance to the serotonin transporter permeation pathway, J. Biol. Chem. 285 (2010) 15369–15379.
[22] D.D.F. Loo, B.A. Hirayama, E.M. Gallardo, J.T. Lam, E. Turk, E.M. Wright, Conformational changes couple Na^+ and glucose transport, Proc. Natl. Acad. Sci. USA 95 (1998) 7789–7794.
[23] D.D. Loo, B.A. Hirayama, M.H. Karakossian, A.K. Meinild, E.M. Wright, Conformational dynamics of hSGLT1 during Na^+/glucose cotransport, J. Gen. Physiol. 128 (2006) 701–720.
[24] X.-Z. Chen, M.J. Coady, J.-Y. Lapointe, Fast voltage clamp discloses a new component of presteady-state currents from the Na^+–glucose cotransporter, Biophys. J. 71 (1996) 2544–2552.
[25] A. Hazama, D.D. Loo, E.M. Wright, Presteady-state currents of the rabbit Na^+/glucose cotransporter (SGLT1), J. Membr. Biol. 155 (1997) 175–186.

[26] T. Liu, D. Krofchick, M. Silverman, Effects on conformational states of the rabbit sodium/glucose cotransporter through modulation of polarity and charge at glutamine 457, Biophys J. 96 (2009) 748–760.
[27] S. Tamura, H. Nelson, A. Tamura, N. Nelson, Short external loops as potential substrate binding site of γ- aminobutyric acid transporters, J. Biol. Chem. 270 (1995) 28712–28715.
[28] M. Grunwald, B.I. Kanner, The accessibility of a novel reentrant loop of the glutamate transporter GLT-1 is restricted by its substrate, J. Biol. Chem. 275 (2000) 9684–9689.
[29] B.P. Krom, S. Juke, Conserved residues R420 and Q428 in a cytoplasmic loop of the citrate/malate transporter CimH of *Bacillus subtilis* are accessible from the external face of the membrane, Biochemistry 42 (2003) 467–474.
[30] D.J. Slotboom, I. Sobczak, W.N. Konings, J.S. Lolkema, A conserved serine rich stretch in the glutamate transporter family forms a substrate-sensitive reentrant loop, Proc. Natl. Acad. Sci. USA 96 (1999) 14282–14287.
[31] D.J. Muller, H. Janovjak, T. Lehto, L. Kuerschner, K. Anderson, Observing structure, function and assembly of single proteins by AFM, Prog. Biophys. Mol. Biol. 79 (2002) 1–43.
[32] T. Puntheeranurak, R.K.H. Kinne, H.J. Gruber, P. Hinterdorfer, Single-molecule AFM studies of substrate transport by using the sodium-glucose cotransporter SGLT1, J. Korean Phys. Soc. 52 (2008) 1336–1340.
[33] N.K. Tyagi, P. Goyal, A. Kumar, D. Pandey, W. Siess, R.K. Kinne, High-yield functional expression of human sodium/D-glucose cotransporter1 in *Pichia pastoris* and characterization of ligand-induced conformational changes as studied by tryptophan fluorescence, Biochemistry 44 (2005) 15514–15524.
[34] F. Castaneda, A. Burse, W. Boland, R.K. Kinne, Thioglycosides as inhibitors of hSGLT1 and hSGLT2: potential therapeutic agents for the control of hyperglycemia in diabetes, Int. J. Med. Sci. 4 (2007) 131–139.
[35] J. Preiner, J. Tang, V. Pastushenko, P. Hinterdorfer, Higher harmonic atomic force microscopy: imaging of biological membranes in liquid, Phys. Rev. Lett. 99 (2007) 046102.
[36] G. Binnig, C.F. Quate, C. Gerber, Atomic force microscope, Phys. Rev. Lett. 56 (1986) 930–933.
[37] H. Dai, J.H. Hafner, A.G. Rinzler, D.T. Colbert, R.E. Smalley, Nanotubes as nanoprobes in scanning probe microscopy, Nature 384 (1996) 147–150.
[38] Y.F. Dufrene, P. Hinterdorfer, Recent progress in AFM molecular recognition studies, Pflugers Arch. 456 (2008) 237–245.
[39] P. Parot, Y.F. Dufrene, P. Hinterdorfer, C. Le Grimellec, D. Navajas, J.L. Pellequer, S. Scheuring, Past, present and future of atomic force microscopy in life sciences and medicine, J. Mol. Recognit. 20 (2007) 418–431.
[40] C. Verbelen, H.J. Gruber, Y.F. Dufrene, The NTA-His6 bond is strong enough for AFM single-molecular recognition studies, J. Mol. Recognit. 20 (2007) 490–494.
[41] A. Ebner, L. Wildling, A.S. Kamruzzahan, C. Rankl, J. Wruss, C.D. Hahn, M. Holzl, R. Zhu, F. Kienberger, D. Blass, P. Hinterdorfer, H.J. Gruber, A new, simple method for linking of antibodies to atomic force microscopy tips, Bioconjug. Chem. 18 (2007) 1176–1184.
[42] A.S. Kamruzzahan, A. Ebner, L. Wildling, F. Kienberger, C.K. Riener, C.D. Hahn, P.D. Pollheimer, P. Winklehner, M. Holzl, B. Lackner, D.M. Schorkl, P. Hinterdorfer, H.J. Gruber, Antibody linking to atomic force microscope tips via disulfide bond formation, Bioconjug. Chem. 18 (2007) 1473–1481.
[43] J. Sotres, A. Lostao, L. Wildling, A. Ebner, C. Gomez-Moreno, H.J. Gruber, P. Hinterdorfer, A.M. Baro, Unbinding molecular recognition force maps of localized single receptor molecules by atomic force microscopy, Chemphyschem 9 (2008) 590–599.
[44] L.A. Chtcheglova, F. Atalar, U. Ozbek, L. Wildling, A. Ebner, P. Hinterdorfer, Localization of the ergtoxin-1 receptors on the voltage sensing domain of hERG K^+ channel by AFM recognition imaging, Pflugers Arch. 456 (2008) 247–254.
[45] L.A. Chtcheglova, J. Waschke, L. Wildling, D. Drenckhahn, P. Hinterdorfer, Nano-scale dynamic recognition imaging on vascular endothelial cells, Biophys. J. 93 (2007) L11–13.
[46] C.K. Riener, C.M. Stroh, A. Ebner, C. Klampfl, A.A. Gall, C. Romanin, Y.L. Lyubchenko, P. Hinterdorfer, H.J. Gruber, Simple test system for single molecule recognition force microscopy, Anal. Chim. Acta 479 (2003) 59–75.
[47] T. Puntheeranurak, L. Wildling, H.J. Gruber, R.K. Kinne, P. Hinterdorfer, Ligands on the string: single molecule AFM studies on the interaction of antibodies and substrates with the Na^+-glucose co-transporter SGLT1 in living cells, J. Cell Sci. 119 (2006) 2960–2967.
[48] T. Puntheeranurak, M. Kasch, X. Xia, P. Hinterdorfer, R.K. Kinne, Three surface subdomains form the vestibule of the Na^+/glucose cotransporter SGLT1, J. Biol. Chem. 282 (2007) 25222–25230.
[49] T. Puntheeranurak, B. Wimmer, F. Castaneda, H.J. Gruber, P. Hinterdorfer, R.K. Kinne, Substrate specificity of sugar transport by rabbit SGLT1: single-molecule atomic force microscopy versus transport studies, Biochemistry 46 (2007) 2797–2804.
[50] M.R. Eftink, Methods of Biochemical Analysis, John Wiley Publishers, New York, 1991, pp. 127–205.
[51] J.R. Lakowicz, Principles of Fluorescence Spectroscopy, Kluwer Academic/Plenum Publishers, 1999, pp. 1–24.
[52] J.R. Lakowicz, Topics in Fluorescence Spectroscopy—Biological Applications, vol. 3, Plenum Publishers, New York, 1992.
[53] M. Raja, N.K. Tyagi, R.K. Kinne, Phlorizin recognition in a C-terminal fragment of SGLT1 studied by tryptophan scanning and affinity labeling, J. Biol. Chem. 278 (2003) 49154–49163.
[54] M. Raja, H. Kipp, R.K. Kinne, C-terminus loop 13 of Na^+-glucose cotransporter SGLT1 contains a binding site for alkyl glucosides, Biochemistry 43 (2004) 10944–10951.
[55] S.T. Chu, H.J. Lin, H.L. Huang, Y.H. Chen, The hydrophobic pocket of 24p3 protein from mouse uterine luminal fluid: fatty acid and retinol binding activity and predicted structural similarity to lipocalins, J. Pept. Res. 52 (1998) 390–397.
[56] M. Raja, R.E.J. Splbrink, B. de Kruijff, J.A. Killian, Phosphatidic acid plays a special role in stabilizing and folding of the tetrameric potassium channel KcsA, FEBS Lett. 581 (2007) 5715–5722.
[57] S. Ozdirekcan, T.K.M. Nyholm, M. Raja, D.T.S. Rijkers, R.M.J. Liskamp, J.A. Killian, Influence of trifluoroethanol on membrane interfacial anchoring interactions of transmembrane α-helical peptides, Biophys. J. 94 (2008) 1315–1325.
[58] N.K. Tyagi, A. Kumar, P. Goyal, D. Pandey, W. Siess, R.K. Kinne, D-Glucose-recognition and phlorizin-binding sites in human sodium/D-glucose cotransporter1 (hSGLT1): a tryptophan scanning study, Biochemistry 46 (2007) 13616–13628.
[59] M.R. Eftink, C.A. Ghiron, Indole fluorescence quenching studies on proteins and model systems: use of the inefficient quencher succinimide, Biochemistry 23 (1984) 3891–3899.
[60] M.R. Eftink, Biophysical and Biochemical aspects of Fluorescence Spectroscopy, Plenum press, New York, 1991, pp. 1–41.
[61] E. London, A.S. Ladokhin, Current Topics in Membranes, vol. 52, Elsevier, San Diego, 2002, pp. 89–115.
[62] A. Chattopadhyay, Biomembrane Structure and Function: The state of the art, Adenine Press, New York, 1992, pp. 153–163.
[63] A. Chattopadhyay, E. London, Parallax method for direct measurement of membrane penetration depth utilizing fluorescence quenching by spin-labeled phospholipids, Biochemistry 26 (1987) 39–45.
[64] A.S. Ladokhin, Evaluation of lipid exposure of tryptophan residues in membrane peptides and proteins, Anal. Biochem. 276 (1999) 65–71.
[65] A. Chattopadhyay, M.G. McNamee, Average membrane penetration depth of tryptophan residues of the nicotinic acetylcholine receptor by the parallax method, Biochemistry 30 (1991) 7159–7164.
[66] A.K. Ghosh, R. Rukmini, A. Chattopadhyay, Modulation of tryptophan environment in membrane-bound melittin by negatively charged phospholipids: implications in membrane organization and function, Biochemistry 36 (1997) 14291–14305.
[67] X. Chen, D.E. Wolfgang, N.S. Sampson, Use of the parallax-quench method to determine the position of the active-site loop of cholesterol oxidase in lipid bilayers, Biochemistry 39 (2000) 13383–13389.
[68] T.S. Ramalingam, P.K. Das, S.K. Podder, Ricin–membrane interaction: membrane penetration depth by fluorescence quenching and resonance energy transfer, Biochemistry 33 (1994) 12247–12254.
[69] P. Meers, Location of tryptophans in membrane-bound annexins, Biochemistry 29 (1990) 3325–3330.
[70] L.A. Chung, J.D. Lear, W.F. DeGrado, Fluorescence studies of the secondary structure and orientation of model ion channel peptide in phospholipids vesicles, Biochemistry 31 (1992) 6608–6616.
[71] M.J. Clague, J.R. Knutson, R. Blumenthal, A. Hermann, Interaction of influenza hemagglutinin amino-terminal peptide with phospholipids vesicles: a fluorescence study, Biochemistry 30 (1991) 5491–5497.
[72] J. Jones, L.M. Gierasch, Effect of charged residue substitutions on the membrane-interactive properties of signal sequence of the *Escherichia coli* LamB protein, Biophys. J. 67 (1994) 1534–1545.
[73] L. Palmer, A.R. Merrill, Mapping the membrane topology of the closed state of colicin E1 channel, J. Biol. Chem. 269 (1994) 4187–4193.
[74] N.D. Ulbrandt, E. London, D.B. Oliver, Deep penetration of a portion of *Escherichia coli* SecA protein into model membrane is promoted by anionic phospholipids and by partial unfolding, J. Biol. Chem. 267 (1992) 15184–15192.
[75] J.H. Kleinschmidt, L.K. Tamm, Time resolved distance determination by tryptophan fluorescence quenching: probing intermediates in membrane protein folding, Biochemistry 38 (1999) 4996–5005.
[76] M. Raja, R.K. Kinne, Interaction of C-terminal loop 13 of sodium-glucose cotransporter SGLT1 with lipid bilayers, Biochemistry 44 (2005) 9123–9129.
[77] E. Turk, C.J. Kerner, M.P. Lostao, E.M. Wright, Membrane topology of the human Na^+/glucose cotransporter SGLT1, J. Biol. Chem. 271 (1996) 1925–1934.
[78] E. Turk, E.M. Wright, Membrane topology motifs in the SGLT1 cotransporter family, J. Membr. Biol. 159 (1997) 1–20.
[79] D.G. Gagnon, A. Holt, F. Bourgeois, B. Wallendorff, M.J. Coady, J.Y. Lapointe, Membrane topology of loop 13–14 of the Na^+/glucose cotransporter (SGLT1): a SCAM and fluorescent labelling study, Biochim. Biophys. Acta 1712 (2005) 173–184.
[80] J. Lin, J. Kormanec, D. Homerova, R.K. Kinne, Probing transmembrane topology of the high-affinity sodium/glucose cotransporter (SGLT1) with histidine-tagged mutants, J. Membr. Biol. 170 (1999) 243–252.
[81] A. Kumar, N.K. Tyagi, E. Arevalo, K.W. Miller, R.K. Kinne, A proteomic study of sodium/D-glucose cotransporter 1 (SGLT1): topology of loop 13 and coverage of other functionally important domains, Biochim. Biophys. Acta 1774 (2007) 968–974.
[82] P. Hinterdorfer, W. Baumgartner, H.J. Gruber, K. Schilcher, H. Schindler, Detection and localization of individual antibody–antigen recognition events by atomic force microscopy, Proc. Natl. Acad. Sci. USA 93 (1996) 3477–3481.
[83] S. Yagur-Kroll, O. Amster-Choder, Dynamic membrane topology of the *Escherichia coli* β-glucoside transporter BglF, J. Biol. Chem. 280 (2005) 19306–19318.
[84] A. Kumar, N.K. Tyagi, R.K.H. Kinne, Ligand-mediated conformational changes and positioning of tryptophans in reconstituted human sodium/D-glucose cotransporter 1 (hSGLT1) probed by tryptophan fluorescence, Biophys. Chem. 127 (2007) 69–77.

[85] B.A. Hirayama, M.P. Lostao, M. Panayotova-Heiermann, D.D. Loo, E. Turk, E.M. Wright, Kinetic and specificity differences between rat, human, and rabbit Na+-glucose cotransporters (SGLT-1), Am. J. Physiol. Gastrointest. Liver Physiol. 270 (1996) G919–G926.
[86] B. Wimmer, M. Raja, P. Hinterdorfer, H.J. Gruber, R.K. Kinne, C-terminal loop 13 of Na^+/glucose cotransporter 1 contains both stereospecific and non- stereospecific sugar interaction sites, J. Biol. Chem. 284 (2008) 983–991.
[87] R. Kinne, Properties of the glucose transport system in the renal brush border membrane, Curr. Top. Membr. Transport 8 (1976) 209–267.
[88] H. Glossmann, D.M. Neville, Phlorizin receptors in isolated kidney brush border membranes, J. Biol. Chem. 247 (1972) 7779–7789.
[89] D.F. Dietrich, Competitive inhibition of intestinal glucose transporter by phlorizin analogs, Arch. Biochem. Biophys. 117 (1966) 248–256.
[90] S. Wielert-Badt, J.T. Lin, M. Lorenz, S. Fritz, R.K. Kinne, Probing the conformation of the sugar transport inhibitor phlorizin by 2D-NMR, molecular dynamic studies, and pharmacophore analysis, J. Med. Chem. 43 (2000) 1692–1698.
[91] S. Wielert-Badt, P. Hinterdorfer, H.J. Gruber, J.T. Lin, D. Badt, B. Wimmer, H. Schindler, R.K. Kinne, Single molecule recognition of protein binding epitopes in brush border membranes by force microscopy, Biophys. J. 82 (2002) 2767–2774.
[92] N. Oulianova, A. Berteloot, Sugar transport heterogeneity in the kidney: two independent transporters or different transport modes through an oligomeric protein 1. Glucose transport studies, J. Membr. Biol. 153 (1996) 181–194.
[93] N. Oulianova, S. Falk, A. Berteloot, Two step mechanism of phlorizin binding to the SGLT1 protein in the kidney, J. Membr. Biol. 179 (2001) 223–242.
[94] B.A. Hirayama, A. Diez-Sampedro, E.M. Wright, Common mechanisms of inhibition for the Na^+/glucose (hSGLT1) and Na^+/Cl^-/GABA (hGAT1) cotransporters, Br. J. Pharmacol. 134 (2001) 484–495.
[95] M. Quick, E.M. Wright, Employing *Escherichia coli* to functionally express, purify, and characterize a human transporter, Proc. Natl. Acad. Sci. USA 99 (2002) 8597–8601.
[96] E. Turk, O. Kim, J. Le Courte, J.P. Whitelegge, S. Eskandari, J.T. Lam, M. Kreman, G.A. Zampighi, K.F. Faull, E.M. Wright, Molecular characterization of *Vibrio parahaemolyticus* Vsglt: a model for sodium-coupled sugar cotransporters, J. Biol. Chem. 275 (2000) 25711–25716.
[97] H. Jung, S. Tebbe, R. Schmid, K. Jung, Unidirectional reconstitution and characterization of purified Na^+/proline transporter of *Escherichia coli*, Biochemistry 37 (1998) 11083–11088.
[98] A. Kumar, N.K. Tyagi, P. Goyal, D. Pandey, W. Siess, R.K.H. Kinne, Sodium-independent low-affinity D-glucose transport by human sodium/D-glucose cotransporter 1: critical role of tryptophan 561, Biochemistry 46 (2007) 2758–2766.
[99] M. Veenstra, E. Turk, E.M. Wright, A ligand-dependent conformational change of the Na^+/galactose cotransporter of *Vibrio parahaemolyticus*, monitored by tryptophan fluorescence, J. Membr. Biol. 185 (2002) 249–255.
[100] J.L. Vazquez-Ibar, L. Guan, M. Svrakic, H.R. Kaback, Exploiting luminescence spectroscopy to elucidate the interaction between sugar and a tryptophan residue in the lactose permease of *Escherichia coli*, Proc. Natl. Acad. Sci. USA 100 (2003) 12706–12711.
[101] F.J. Sharom, P.L. Russell, Q. Qu, and P. Lu, Fluorescence techniques for studying membrane transport proteins: The P-glycoprotein multidrug transporter, Methods in Molecular Biology, vol. 227: Membrane Transporters: Methods and Protocols, Humana Press Inc., Totowa, NJ.
[102] R. Novakova, D. Homerova, R.K.H. Kinne, E. Kinne-Saffran, J.T. Lin, Identification of a region critically involved in the interaction of phorizin with the rabbit sodium–D-glucose cotransporter SGLT1, J. Membr. Biol. 184 (2001) 55–60.
[103] B. Cheskis, L.P. Freedman, Modulation of nuclear receptor interactions by ligands: kinetic analysis using surface plasmon resonance, Biochemistry 35 (1996) 3309–3318.
[104] A. Szabo, L. Stolz, R. Granzow, Surface plasmon resonance and its use in bimolecular interaction analysis (BIA), Curr. Opin. Struct. Biol. 5 (1995) 699–705.
[105] W. Wang, D.K. Smith, K. Moulding, H.M. Chen, The dependence of membrane permeability by the antibacterial peptide cecropin B and Its analogs, CB-1 and CB-3, on liposomes of different composition, J. Biol. Chem. 273 (1998) 27438–27448.
[106] A. Yamashita, S.K. Singh, T. Kawate, Y. Jin, E. Gouaux, Crystal structure of a bacterial homologue of Na^+/Cl^--depnednet neurotransmitter transporters, Nature 437 (2005) 215–223.
[107] J.W. Bowie, Flip-flopping membrane proteins, Nat. Struct. Mol. Biol. 13 (2006) 94–96.
[108] C. Hunte, E. Screpanti, M. Venturi, A. Rimon, E. Padan, H. Michel, Structure of a Na^+/H^+ antiporter and insights into mechanism of action and regulation by pH, Nature 435 (2006) 1197–1202.
[109] M.S. Sujatha, P.V. Balaji, Identification of common structural features of binding sites in galactose-specific proteins, Proteins 55 (2004) 44–65.
[110] M. Panayotova-Heiermann, D.D. Loo, J.T. Lam, E.M. Wright, Neutralization of conservative charged transmembrane residues in the Na^+/glucose cotransporter SGLT, Biochemistry 37 (1998) 10522–10528.
[111] S.Y. Noskov, B. Roux, Control of ion selectivity in LeuT: two Na^+ binding sites with two different mechanisms, J. Mol. Biol. 377 (2008) 804–818.
[112] S. Ressl, A.C. Terwisscha van Scheltinga, C. Vonrhein, V. Ott, C. Ziegler, Molecular basis of transport and regulation in the Na^+/betaine symporter BetP, Nature 458 (2009) 47–52.